SDRP Journal of Cellular and Molecular Physiology

SAPIENS MTDNA CIRCULAR LONG-RANGE NUMERICAL META-STRUCTURES ARE HIGHLY CORRELATED WITH MTDNA DISEASES MUTATIONS

Research

AUTHOR: Dr Jean-claude PEREZ June 2017

Received Date: 04th May 2017
Accepted Date: 10th June 2017
Published Date:25th June 2017

Dr Jean-claude PEREZ, retired interdisciplinary researcher (IBM),
7 avenue de terre-rouge F33127 Martignas Bordeaux metropole France
CORRESPONDENCE AUTHOR
Dr Jean-claude PEREZ
Email: jeanclaudeperez2@gmail.com jeanclaudeperez3@free.fr

CONFLICTS OF INTEREST
There are no conflicts of interest for any of the authors.

ABSTRACT
Using the circular nature of the 16kbase-pairs human mtDNA genome, we are looking for hypothetical proportions between the C + A and T + G bases. Remarkable proportions are thus discovered, the length of which may be much greater than the length of the genome. We then analyze the impact of evolution on these "numerical resonances" by comparing the referenced mtDNAs of Sapiens, Neanderthal and Denisova. Then, by analyzing 250 characteristic mutations associated with various pathologies, we establish a very strong formal causal correlation between these numerical metastructures and these referenced mutations.
To summarize, we should think then research on the following situation:
Inputs: 250 cases of mtDNA mutations associated with various human diseases.
An operator: The exhaustive search for mtDNA genome "Fibonacci resonances" associated with these mutations.
A "binary" output: a common behavior of the mtDNA genome resulting from these 250 mutations disorders.

INTRODUCTION
Nearly 30 years ago, when we were just starting to have available genes and small genomes DNA sequences of viruses or bacteria, while the large project of human genome sequencing was just beginning, we showed the existence of specific numerical nucleotides proportions in the DNA of the genes (1, 2). This discovery also applied to small circular genomes such as those of bacteria or mitochondrial DNA genes-rich sequences. On the other hand, it did not work for non-coding DNA sequences regions like human chromosomes.
In the cells, Mitochondria are known as the powerhouses of the cell. They are organelles that act like a digestive system which takes in nutrients, then breaks them down, and creates energy rich molecules for the cell. The biochemical processes of the cell are known like a « cellular respiration ».
The genome of the mitochondria or "mtDNA" is a small 16kb genome whose remarkable feature is the fact that it is looped back on itself forming a circular sequence. This is also true of the genomes of most bacteria. As in prokaryotes, there is a very high proportion of coding DNA and an absence of repeats. It encodes 37 genes: 13 for subunits of respiratory complexes I, III, IV and V, 22 for mitochondrial tRNA (for the 20 standard amino acids, plus an extra gene for leucine and serine), and 2 for rRNA. One mitochondrion can contain two to ten copies of its DNA.
Mitochondrial genomes have been extensively studied and identified, especially for many years by Douglas C. Wallace (3, 4, 5). This genome possesses the remarkable hereditary characteristic of being transmitted only

by the mother (6), which makes it a privileged tool in the evolution studies of human species. Various heterogeneous genomes copies can be found in the same cell, it is heteroplasmia (7). It would also appear that the genome of mitochondria and its mutations can play an important role in aging (8, 9). But, above all, simple mutations associated with various diseases (such as LHON) are observed, and somatic mutations are

1.This scientific paper is the first in a series of 6 articles demonstrating the existence of global numerical structures on the scale of whole human chromosomes and genomes. Particularly, the method of analysis of fractal periods will be completely studied in: « DUF1220 Homo sapiens fractal periods architectures breakthrough » and in "Humans and Primates Chromosomes4 Fractal CODES: periodic stationnary waveforms charaterizing and differenciating Neanderthal and Sapiens whole chromosomes DNA sequences". The three other articles will be: "Global and long range fractal differences between sapiens and neanderthal genomes" and "The Human Genome Optimum : a numerical universal law controling all LOH chromosomal deletions involved in human cancers " and « Fractal Chaos » : from Artificial Intelligence Neural Networks to Human Chromosomes DNA sequences Hidden Codes: Self-similarity and Scale Invariance...

2.Einstein's citation reported in the book Theory I: The mental representation of the Universe (English Edition) Format Kindle, by Lepeltier P . and Lepeltier F. , https://www.amazon.fr/Theory-mental-representation-Universe-English-ebook/dp/B013NP08RI/ref=asap_bc?ie=UTF8

found in cells associated with various diseases such as cancers (10). Effectvely, It is now emerging that somatic mutations in mitochondrial DNA (mtDNA) are also linked to other complex traits, including neurodegenerative diseases, ageing and cancer.

METHODS :

1. The method of analysis:

The particular proportions that we are looking for here revolve around the numbers of Fibonacci and Lucas:
The Fibonacci numbers sequence: 0 1 1 2 3 5 8 13 21 34 55 89 144 233 377 610 987 1597 2584 4181 **6765 10946 17711** 28657 46368 75025 121393 196418 317811
The Lucas numbers sequence : 2 1 3 4 7 11 18 29 47 76 123 199 322 521 843 1364 2207 3571 5778 9349 15127 24476 39603
The specific proportions that we will search will be established as follows:
From each base of the circular genome,
Delimiting a region of length F (i),
If in this region we find F (i-1) bases C or A;
Then we will say we have discovered a "resonance".
Consequently, this subsequence will also contain F (i-2) bases T + G.

For example, From
base 10000,
We analyze the subsequence of the following 17711 nucleotides (considering the genome looped on itself thus of an "infinite" length).
Then, if we find within this sequence exactly 10946 bases C or A, And,
consequently, 6765 bases T or G,

Then we declare to have discovered a *"resonance of length 17711"*.

2. The different genomes analyzed:

Reference Sapiens mtDNA genome called *"Cambridge revised"*. It is found inThe rCRS is GenBank number **NC_012920**. Click here for details. 3
Reference Neanderthal1 mtDNA genome (11) : from
https://www.ncbi.nlm.nih.gov/pmc/articles/PMC2602844/
References DENISOVA1 and DENISOVA2 mtDNA genomes (12) : from
https://www.ncbi.nlm.nih.gov/pmc/articles/PMC4697428/
Details :
DENISOVA1 alias « Denisova8 » in the original paper:
Select item 9529523511. Homo sapiens ssp. Denisova isolate Denisova8 mitochondrion, complete genome 16,573 bp circular DNA Accession: KT780370.1 GI: 952952351
DENISOVA2 alias « ALTAI » in the original paper:
Select item 2926064082. Homo sp. Altai mitochondrion, complete genome 16,570 bp circular DNA Accession: NC_013993.1 GI: 292606408

Reference Chimpanzee mtDNA genome : from https://www.ncbi.nlm.nih.gov/nuccore/1262390
>X93335.1 Pan troglodytes mitochondrial DNA, complete genome (isolate Jenny)

3. The different diseases mutations analyzed:
They will be found in http://www.mitomap.org/MITOMAP .

3**The revised Cambridge Reference Sequence (rCRS) is GenBank number NC_012920**.
Please use this new number when citing the rCRS in publications. The rCRS is a reference sequence, not a "consensus" sequence. It is a single reference individual from haplogroup H2a2 and has been used as a standard for reporting variants for over 30 years.

RESULTS :

1/ Evolution considerations comparing 5 humanoids mtDNA genomes : Recall
Fibonacci numbers sequence:

0 1 1 2 3 5 8 13 21 34 55 89 144 233 377 610 987 1597 2584 4181 6765 10946 17711 28657 46368 75025 121393 196418 317811

	Genome length (bases pairs)	Number of Resonance 10946 6765 C+A 4181 T+G	Number of Resonance 17711 10946 C+A 6765 T+G	Number of Resonance 28657 17711 C+A 10946 T+G	Number of Resonance 46368 28657 C+A 17711 T+G	Number of Resonance 75025 46368 C+A 28657 T+G
sapiens	16568	10	8	152	0	0
neander-thal1	16565	2	16	23	92	0
denisova1	16573	52	33	41	36	0
denisova2	16570	10	62	10	68	0
Chimp	16561	33	76	33	46	0

Table 1 : Table comparing (C+A) / TCAG long range Fibonacci resonances for 5 reference humanoids mtDNA genomes

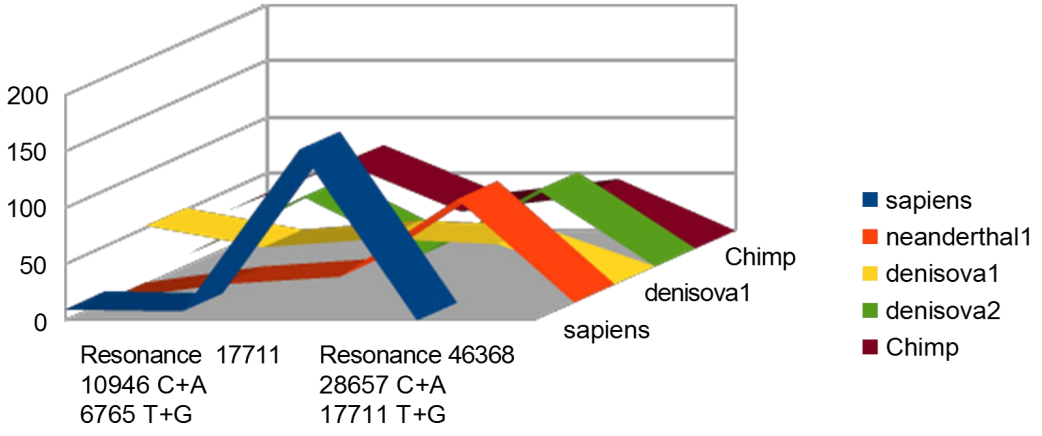

Figure 1 : graph comparing (C+A) / TCAG long range Fibonacci resonances for 5 reference humanoids mtDNA genomes

It is observed that, unlike Sapiens, the four ancestral genomes in the Evolution are characterized by long circular resonances of 46,368 bases. Contrarly Sapiens is characterized by a number of 28657 bases long resonances very superior (152 resonances).
We will now analyze the impact of mutations on the resonances for 3 types of situations representing a total of 150 diseases related mutations.

2. Analysing 20 mtDNA mutations with reports of disease associations :
Datas from MITOMAP database :

Organized by mtDNA location:

UPDATED rRNA/tRNA Mutations

UPDATED Coding & Control Region Mutations

Source web access : http://www.mitomap.org/foswiki/bin/view/MITOMAP/MutationsRNA

582	MT-TF	Mitochondrial myopathy	T582C	tRNA Phe	-	+	Reported	0
583	MT-TF	MELAS / MM & EXIT	G583A	tRNA Phe	-	+	Cfrm	0
586	MT-TF	Extrapyramidal disorder with akinesia-rigidity, psychosis and SNHL	G586A	tRNA Phe	-	+	Reported	0
602	MT-TF	Axial myopathy with encephalopathy	C602T	tRNA Phe	-	+	Reported	0
606	MT-TF	Myoglobinuria	A606G	tRNA Phe	+	+	Unclear	13
608	MT-TF	Tubulo-interstitial nephritis	A608G	tRNA Phe	+	-	Reported	0
611	MT-TF	MERRF	G611A	tRNA Phe	-	+	Reported	0
616	MT-TF	Maternally inherited epilepsy	T616C	tRNA Phe	+	+	Reported	1
616	MT-TF	Maternally inherited epilepsy	T616G	tRNA Phe	+	+	Reported	1
617	MT-TF	Carotid artery stenosis	G617A	tRNA Phe	-	+	Reported	0
618	MT-TF	MM	T618C	tRNA Phe	-	+	Reported	0
618	MT-TF	Ptosis CPEO MM & EXIT	T618G	tRNA Phe	-	+	Reported	0
622	MT-TF	EXIT & Deafness	G622A	tRNA Phe	-	+	Reported	0
625	MT-TF	SNHL & Epilepsy	G625A	tRNA Phe	-	+	Reported	0
628	MT-TF	DEAF	C628T	tRNA Phe	-	+	Reported	3
636	MT-TF	DEAF	A636G	tRNA Phe	+	-	Reported	7
642	MT-TF	Ataxia, PEO, deafness	T642C	tRNA Phe	-	+	Reported	0
663	MT-RNR1	Coronary Atherosclerosis risk	A663G	12S rRNA	+	-	Reported	943
669	MT-RNR1	DEAF	T669C	12S rRNA	+	-	Reported	66
721	MT-RNR1	Possibly LVNC-associated	T721C	12S rRNA	+	-		

Table 2 : Detail of 20 cases of reported mitochondrial DNA base substitution diseases: rRNA/tRNA mutations

Location mutation	Number of Resonance 10946 6765 C+A 4181 T+G reference 10 resonances	Number of Resonance 17711 10946 C+A 6765 T+G reference 8 resonances	Number of Resonance 28657 17711 C+A 10946 T+G reference 152 resonances
582	16	13	150
583	16	13	150
586	16	13	150
602	18	13	143
606	18	13	145
608	18	13	143
611	16	13	150
616	16	13	150
616	10	8	152
617	16	13	150
618	16	13	150
618	10	8	152
622	16	13	150
625	16	13	150
628	18	13	142
636	18	13	142
642	16	13	149
663	18	13	142
669	16	13	148
721	16	13	151

Table 3: Table results for 20 cases of Reported Mitochondrial DNA Base Substitution Diseases: rRNA/tRNA mutations

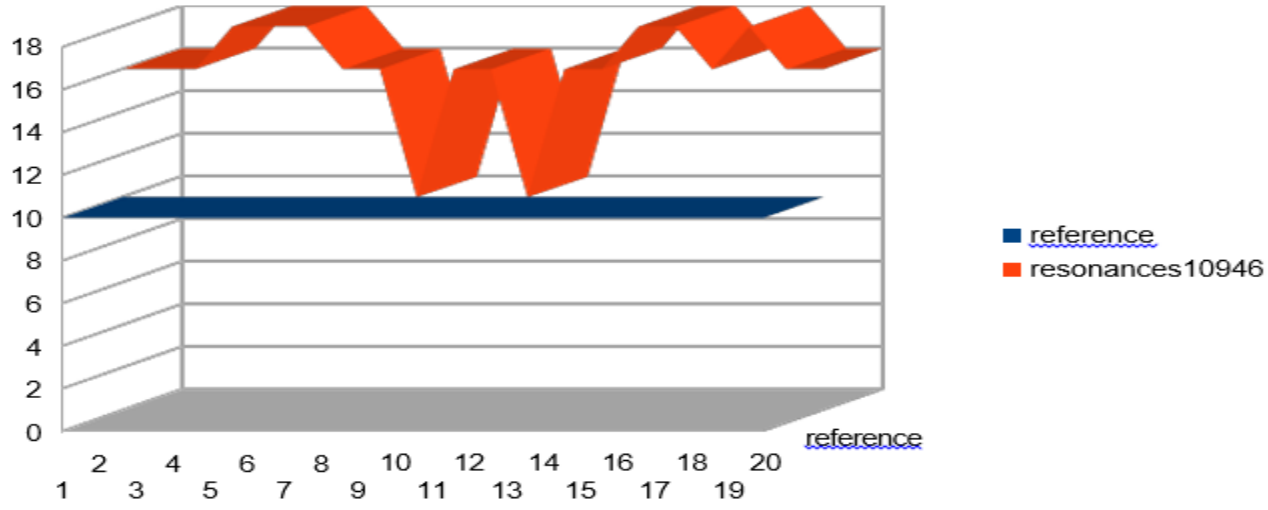

Figure 2 : Resonances 10946 for 20 cases of Reported Mitochondrial DNA Base Substitution Diseases: rRNA/tRNA mutations.

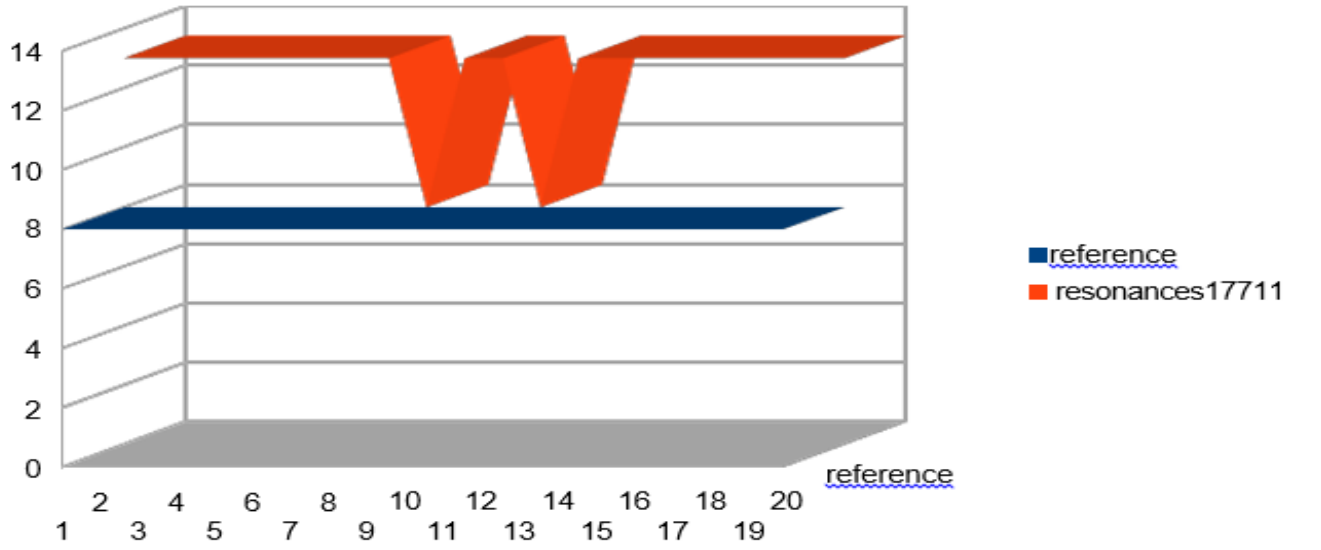

Figure 3 : Resonances 17711 for 20 cases of Reported Mitochondrial DNA Base Substitution Diseases: rRNA/tRNA mutations.

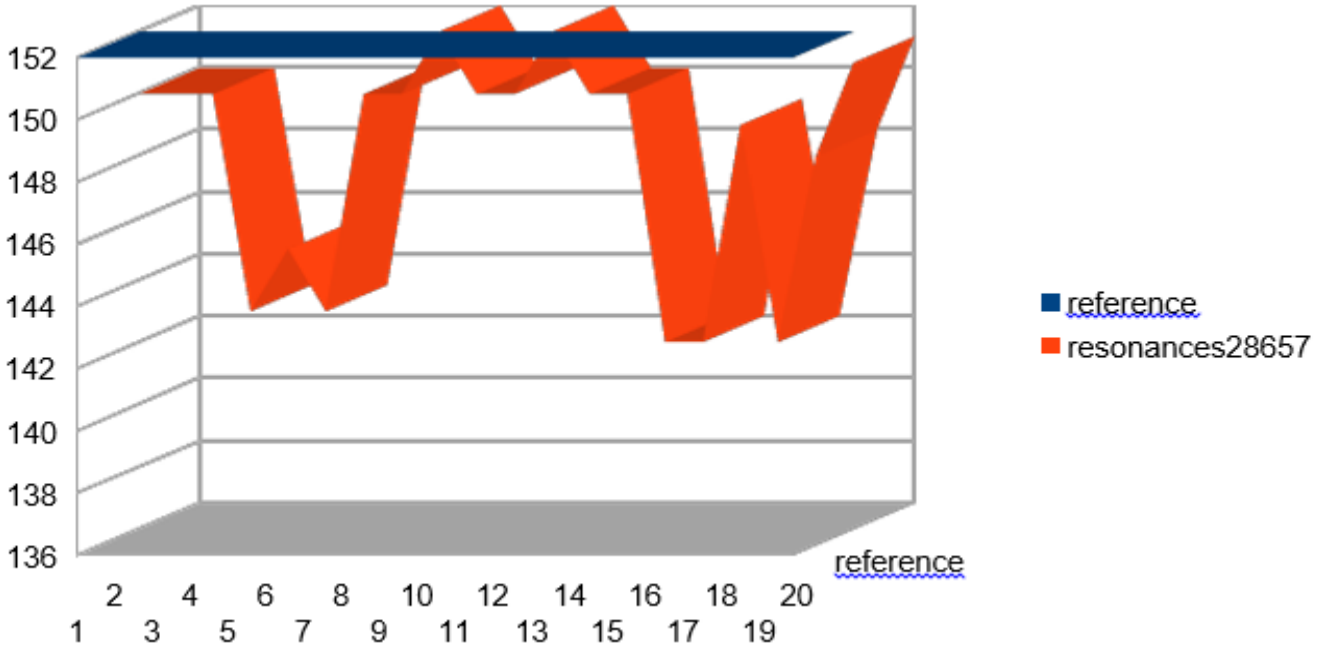

Figure 4 : Resonances 28657 for 20 cases of Reported Mitochondrial DNA Base Substitution Diseases: rRNA/tRNA mutations.

It is noted that the resonances 10946 and 17711 INCREASE in the cases of mutations whereas the very long resonances 28657 DECREASE in the cases of mutations.

3. Analysing 44 (25+19) mtDNA somatic mutations from 2 different mtDNA genome regions : The 25 first cases :

Locus	Nucleotide Position	Nucleotide Change	Homoplasmy	Hetero-plasmy	Cell or Tissue Type	GB Sequences (# FL / # CR)*	References
MT-DLOOP	1	G-C	+	-	prostate tumor	-	references
MT-DLOOP	32	A-G	-	+	POLG/PEO patient	-	references
MT-DLOOP	45	A-G	-	+	control skeletal muscle	1 (1/0)	references
MT-DLOOP	46	T-C	-	+	control skeletal muscle	3 (2/1)	references
MT-DLOOP	52	T-C	+	-	ovarian tumor	13 (1/12)	references
MT-DLOOP	55	T-C	-	+	control skeletal muscle	111 (64/47)	references
MT-DLOOP	59	T-C	-	+	control skeletal muscle	55 (41/14)	references
MT-DLOOP	60	T-C	-	+	normal tissues	31 (18/13)	references
MT-DLOOP	62	G-C	-	+	aging brains	47 (46/1)	references
MT-DLOOP	64	**C-A**	-	+	POLG/PEO muscle, normal tissues	3 (2/1)	references
MT-DLOOP	64	C-T	-	+	aging brains	1576 (948/628)	references
MT-DLOOP	66	G-del	-	+	normal tissues	35 (20/15)	references
MT-DLOOP	66	G-A	-	+	POLG/PEO muscle, normal tissues	59 (19/40)	references
MT-DLOOP	67	G-A	-	+	POLG/PEO muscle, normal tissues	1 (0/1)	references
MT-DLOOP	72	T-C	-	+	aging brains, POLG/PEO & control muscle, normal tissues	954 (553/401)	references
MT-DLOOP	73	A-G	+	+	aging brains, POLG/PEO & control muscle, buccal cell, thyroid & prostate tumors	44239 (23631/20608)	references
MT-DLOOP	74	G-A	+	-	head/neck tumor	-	references
MT-DLOOP	74	T-A	-	+	POLG/PEO muscle	-	references
MT-DLOOP	74	**T-G**	-	+	POLG/PEO muscle	1 (0/1)	references
MT-DLOOP	80	**C-A**	-	+	POLG/PEO muscle	-	references
MT-DLOOP	84	A-G	-	+	POLG/PEO muscle	-	references
MT-DLOOP	91	C-T	-	+	control skeletal muscle	4 (4/0)	references
MT-DLOOP	92	G-A	-	+	aging brains	107 (101/6)	references
MT-DLOOP	94	G-A	+	-	prostate tumor, normal tissues	311 (126/185)	references
MT-DLOOP	97	G-A	-	+	POLG/PEO muscle	20 (17/3)	references
MT-DLOOP	98	C-del	+	-	thyroid tumor	-	references
MT-DLOOP	100	G-A	-	+	POLG/PEO muscle	1 (0/1)	references

Table 4: Table of 25 mtDNA somatic mutations.

The 19 other cases :
http://www.mitomap.org/foswiki/bin/view/MITOMAP/MutationsSomatic

Position	Locus	Nucleotide Change	Amino Acid Change	Homoplasmy	Heteroplasmy	Cell or Tissue type	Note	References
16537		C-T	non-coding	+	-	pancreatic cancer	.	1
16532		A-T	non-coding	-	+	bladder tumor		1
16527		C-T	non-coding	+	-	pancreatic cancer cell line	.	1
16519		T-C	non-coding	+	+	glioblastoma, gastric, lung, ovarian, prostate tumors	.	6
16474		G-C	non-coding	-	+	prostate tumor	.	2
16465		C-T	non-coding	+	-	ovarian tumor	.	1
16459		C-T	non-coding	+	-	prostate tumor	.	2
16438		G-A	non-coding	-	+	gastric carcinoma	.	1
16403		C-T	non-coding	+	-	prostate tumor	.	2
16399		A-G	non-coding	-	+	gastric carcinoma	.	1
16391		G-A	non-coding	+	-	ovarian tumor		1
16390		G-A	non-coding	+	+	breast, ovarian tumor	.	2
16365		C-T	non-coding	+	-	ovarian	.	2
16357		T-C	non-coding	+	-			1
16356		T-C	non-coding	+	-	glioblastoma	.	2
16355		C-T	non-coding	+	+	normal tissues	.	2
16352		T-C	non-coding	-	+	MNGIE fibroblasts	.	1
16324		T-C	non-coding	+	-	esophageal cancer	.	1
16311		T-C	non-coding	-	+	prostate tumor	.	1

Table 5: Table of 19 mtDNA somatic mutations.

Location mutation	Number of Resonance 10946 6765 C+A 4181 T+G reference 10 resonances	Number of Resonance 17711 10946 C+A 6765 T+G reference 8 resonances	Number of Resonance 28657 17711 C+A 10946 T+G reference 152 resonances
1	16	13	152
32	18	13	145
45	18	13	145
46	16	13	152
52	16	13	152
55	16	13	152
59	16	13	152
60	16	13	152
62	16	13	152
64	10	8	152
64	18	13	145
66	16	13	152
67	16	13	152
72	16	13	152
73	18	13	145
74	16	13	152
74	16	13	152
74	10	8	152
80	10	8	152
84	18	13	145
91	18	13	145
92	16	13	152
94	16	13	152
97	16	13	152
100	16	13	152
16536	18	13	145
16531	18	13	145
16526	18	13	145
16518	16	13	152
16473	16	13	154
16464	18	13	147
16458	18	13	147
16437	16	13	154
16402	18	13	147
16398	18	13	147
16390	16	13	154
16389	16	13	154
16364	18	13	147
16356	16	13	154
16355	16	13	154
16354	18	13	147
16351	16	13	154
16323	16	13	154
16310	16	13	154

Table 6: Results of 44 (25+19) mtDNA somatic mutations.

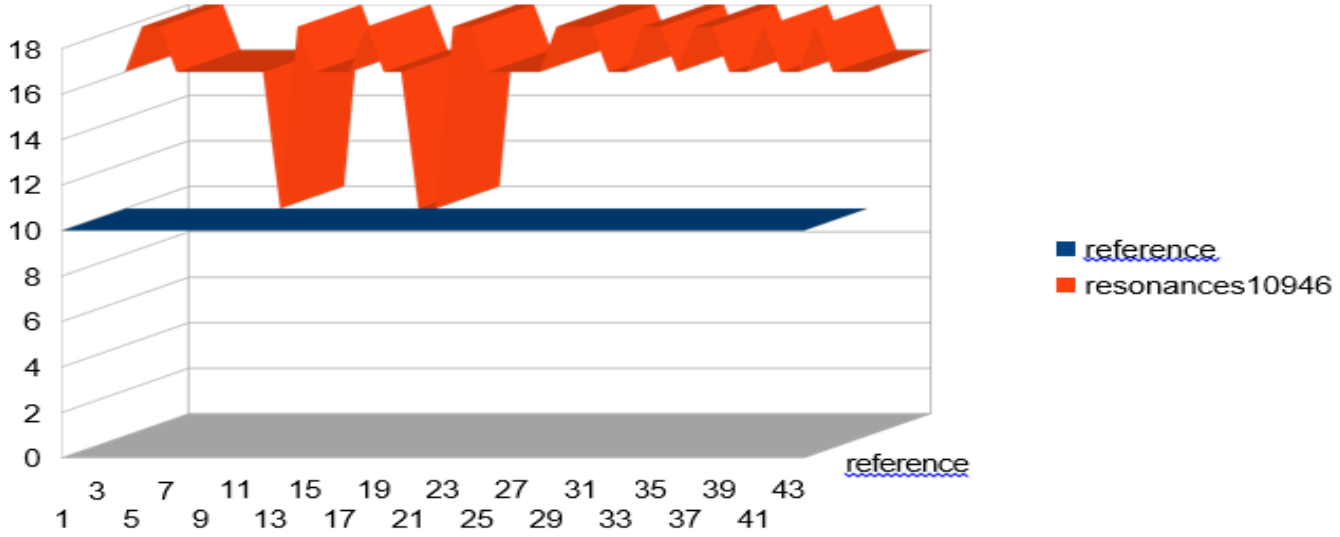

Figure5 : graphic of resonances 10946 for 44 (25+19) mtDNA somatic mutations.

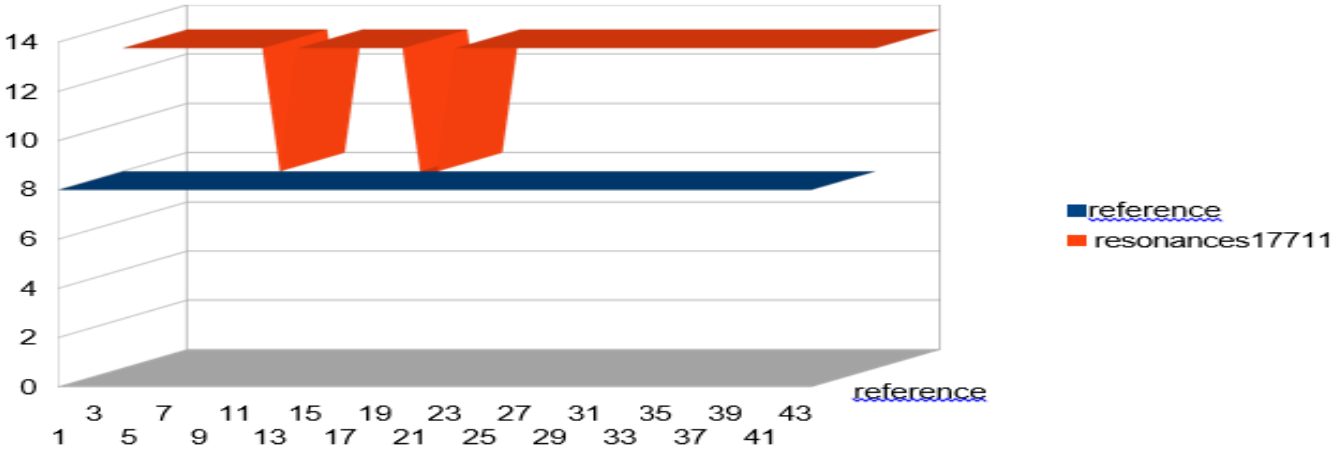

Figure 6 : graphic of resonances 17711 for 44 (25+19) mtDNA somatic mutations.

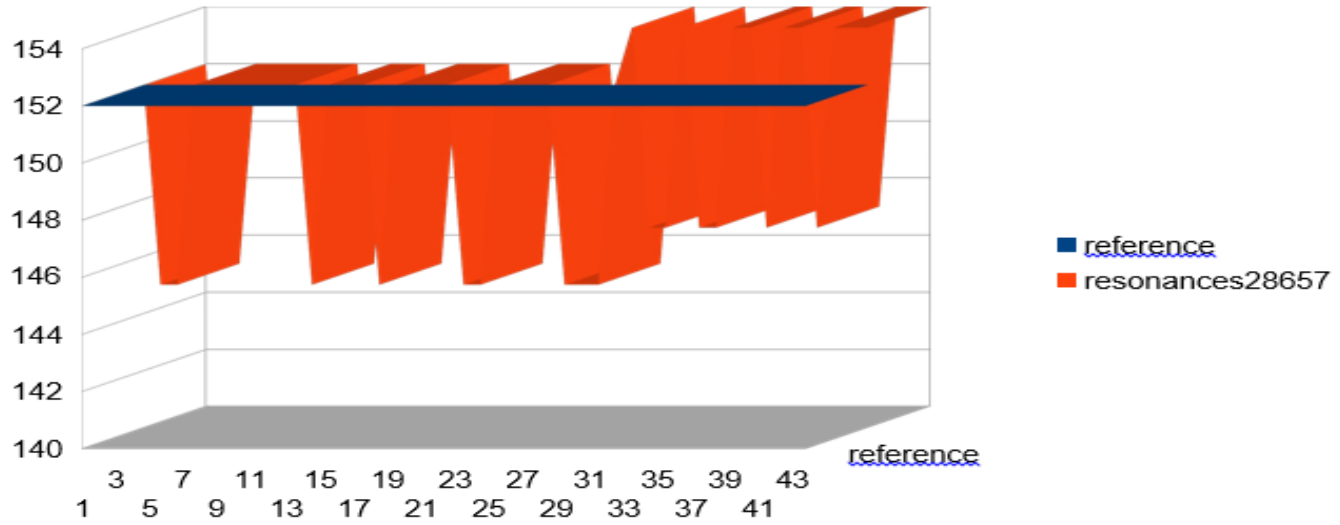

Figure 7 : graphic of resonances 28657 for 44 (25+19) mtDNA somatic mutations.

It is also noted here that the resonances 10946 and 17711 INCREASE in the case of mutations whereas the very long resonances 28657 DECREASE most often in the cases of mutations.

4. Analysing all LHON disease mtDNA mutations :
We will now analyze 18 + 18 = 36 cases of mutations associated with LHON (Leber's Hereditary Optic Neuropathy):

Sources :
http://www.mitomap.org/foswiki/bin/view/MITOMAP/MutationsLHON

Mutation	Nt Δ	AA Δ	AA Cons a	% Patients	% Controls	Het. b	Penetrance c % Relatives	Penetrance c % Males	% Recovery d	Referen
D4*LHON11778A	**G-A**	**R340H**	**H**	**69**	**0**	**+/-**	**33-60**	**82**	**4**	*(27)*
D1*LHON3460A	**G-A**	**A52T**	**M**	**13**	**0**	**+/-**	**14-75**	**40-80**	**22**	*(10, 1*
D6*LHON14484C	**T-C**	**M64V**	**L**	**14**	**0**	**+/-**	**27-80**	**68**	**37-65**	*(2, 13,*
D1*LHON-A3376A	G-A	E24K	H	Rare	0	+/+	NA	NA	NA	*(33, 34,*
D1*LHON3635A	G-A	S110N	H	Rare	0	+/-	29 (range 11-64)	54 (range 25-100)	Low	*(3)*
D1*LDYT3697A	G-A	G131S	H	Rare	0	+/+	NA	NA	NA	*(32)*
D1*LHON3700A	G-A	A112T	H	Rare	0	-	NA	NA	UN	*(1a, 7*
D1*LHON3733A	G-A	E143K	H	Rare	0	+/-	24-30	36-44	Yes	*(1a, 2*
D1*LHON4171A	C-A	L289M	H	Rare	0	+/-	46	47	Yes	*(20)*
D3*LDYT10197A	G-A	A47T	H	Rare	4/30589	+/+	NA	NA	NA	*(36)*
D4L*LHON10663C	T-C	V65A	L	Rare	0	+/-	56	60	UN	*(1a, 1*
D5*LHON13051A	G-A	G239S	H	Rare	0	-	56	63	UN	*(5b, 1*
D6*LDYT14459A	G-A	A72V	M	Rare	0	+	NA	NA	Low	*(8, 19,*
D6*LHON14482A	C-A	M64I	L	Rare	0	+/-	NA	89	Yes	*(1a, 2*
D6*LHON14482G	C-G	M64I	L	Rare	0	-	NA	NA	UN	*(11)*
D6*LHON14495G	A-G	L60S	H	Rare	0	+	NA	NA	Low	*(4)*

D6*LHON14502C	T-C	I58V	H	Rare	0	-	14502:10% 14502+11778: 37%	14502:11% 14502+11778: 47%	UN	*(1a, 30,*
D6*LHON14568T	C-T	G36S	M	Rare	0	-	NA	NA	UN	*(6, 28*

Table 7 : First set of candidate LHON mutations found as single family or singleton cases

B. Other candidate LHON mutations found as single family or singleton cases

Mutation	Nt Δ	AA Δ	AA Cons a	# Patients	# Controls	Het. b	Recovery d	References
MTND1*LHON3472T	T-C	F56L	H	1 case	3/18037		UN	*(22b)*
MTND1*LHON4025T	C-T	T240M	M	1 family; 3 cases	0	_	UN	*(15)*
MTND2*LHON5244A	G-A	G259S	H	1 case	0	+	UN	*(1b)*
MTND2*LHON4640A	C-A	I57M	L	1 family; 4 cases	0	_	UN	*(3)*
MTND3*LHON10237C	T-C	I60T	H	1 family; 2 cases	0	_	UN	*(9)*
MTND4*LHON11253C	T-C	I165T	H	1 case	0	_	Yes	*(22)*
MTND4*LDYT11696G/ MTND6*LDYT14596A	**A-G** **G-A**	V312I I26M	L M	1 family; 11 cases	0	+	UN	*(5)*
MTND5*LHON12811C	T-C	Y159H	M	1 family; 2 cases	0	_	UN	*(15)*
MTND5*LHON12848T	C-T	A171V	H	1 case	0	+	UN	(23)
MTND5*LHON13637G	A-G	Q434R	L	1 family; 3 cases	0	_	UN	*(15)*
MTND5*LHON13730A	G-A	G465E	M	1 case	0	+	Yes	*(12)*
MTND6*LHON14279A	G-A	S132L	M	1 family; 2 cases	0	_	UN	*(29)*
MTND6*LHON14325C	T-C	N117D	L	1 case	0	_	UN	*(14)*
MTND6*LHON14498T	**C-T**	Y59C	M	1 case	0	+/_	UN	*(28)*
MTATP6*LHON9101C	T-C	I192T	L	1 case	0	_	UN	*(21)*
MTCO3*LHON9804A	G-A	A200T	H	Multiple unrelated singleton cases	0	_	UN	*(14, 17)*
MTCYB*LHON14831A	G-A	A29T	M	1 case	0	_	UN	*(7)*

Table 8 : Other candidate LHON mutations found as single family or singleton cases.

Location mutation	Number of Resonance 10946 6765 C+A 4181 T+G reference 10 resonances	Number of Resonance 17711 10946 C+A 6765 T+G reference 8 resonances	Number of Resonance 28657 17711 C+A 10946 T+G reference 152 resonances
11777	11	13	187
3459	17	13	148
14483	15	13	193
3375	17	13	148
3634	17	13	148
3696	17	13	148
3699	17	13	148
3732	17	13	148
4170	10	8	152
10196	11	13	148
10662	11	13	144
13050	11	13	193
14458	12	13	193
14481	10	8	152
14481	19	13	172
14494	18	13	172
14501	16	13	193
14567	18	13	172
3471	17	13	148
4024	19	13	179
5243	17	13	148
4639	10	8	152
10236	11	13	148
11252	11	13	154
11695	11	13	169
14595	18	13	172
12810	11	13	190
12847	11	13	211
13636	11	13	172
13729	11	13	193
14278	10	13	193
14324	10	13	193
14497	16	13	193
9100	11	13	148
9803	11	13	148
14830	16	13	197

Table 9 : Results for 36 mutations cases of LHON disease (Leber's Hereditary Optic Neuropathy).

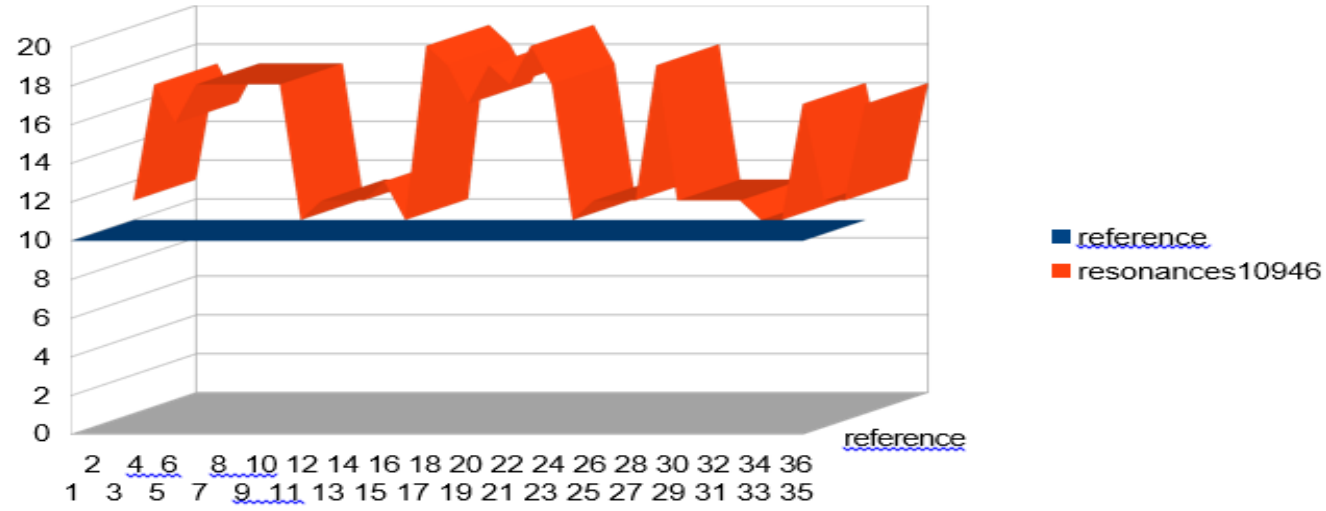

Figure 8 : Graphics related 10946 resonances for 36 cases of mutations associated with the LHON disease (Leber's Hereditary Optic Neuropathy).

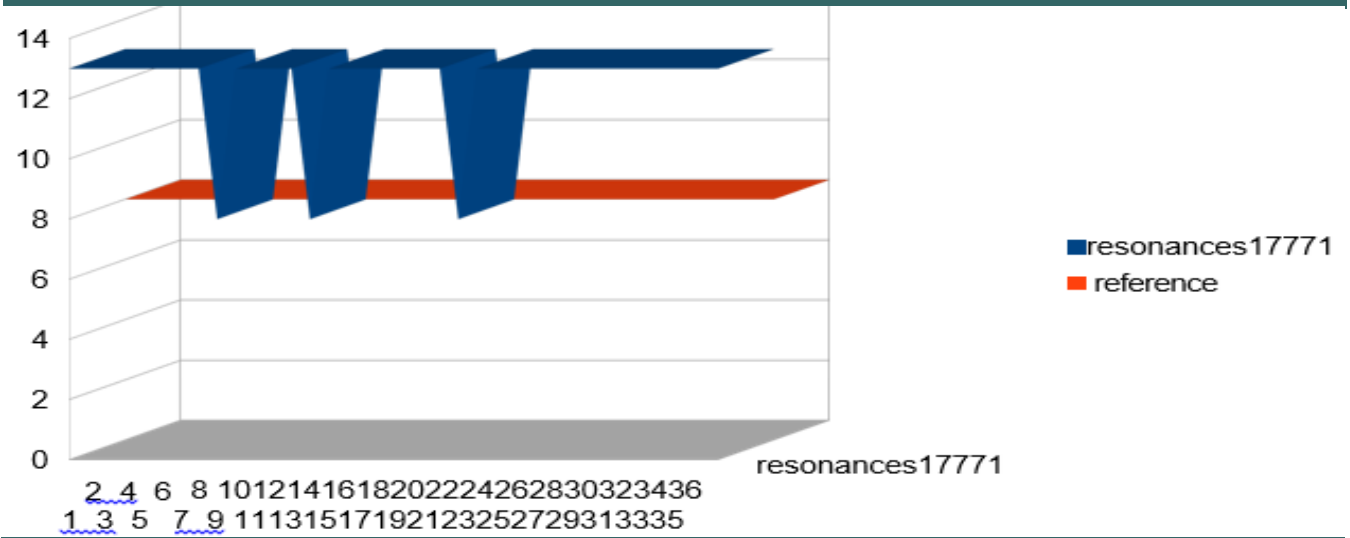

Figure 9 : Graphics related 17771 resonances for 36 cases of mutations associated with the LHON disease (Leber's Hereditary Optic Neuropathy).

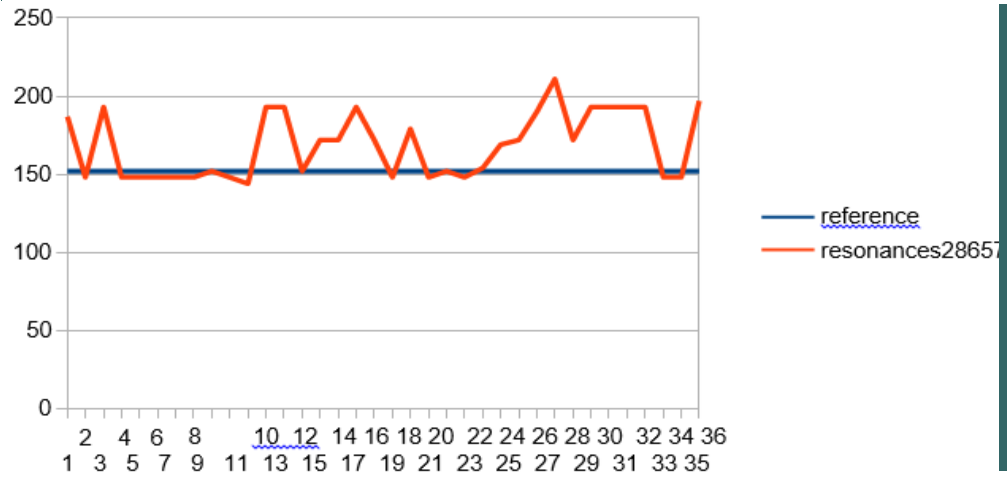

Figure 10: Detail of graphics related 28657 resonances for 36 cases of mutations associated with the LHON disease (Leber's Hereditary Optic Neuropathy).

It is noted that the resonances 10946 and 17711 INCREASE in all the cases of mutations whereas the very long resonances 28657 DECREASE in the majority of the mutations cases.

DISCUSSION :

1. Synthesis :

	Number of Resonances 10946			Number of Resonances 17711			Number of Resonances 28657		
	decrease	neutral	increase	decrease	neutral	increase	decrease	neutral	increase
1/ 20 disease mutations	0	2	18	0	2	18	18	2	0
2/ 44 somatic mutations	0	3	41	0	3	41	32	3	9
3/ all 36 LHON mutations	0	3	33	0	3	33	13	3	20
Cumul by 100	0	8	92	0	8	92	63	8	29
Score = (increase +neutral) / (total)	100,00%			100,00%			37.00%		
Score = (decrease) / (total)	0,00%			0,00%			63.00%		

Table 10 : Synthesis of the cumulate 150 mutations cases.

Note: "neutral" mutations have no effect because they result from mutations T <==> G or A <==> C.

It is finally observed that all 150 mutations increase or retain resonances 10946 and 17711 (100%) while they decrease more generally the very long resonances 28657(63%).

2. lucas verification extension:

The sequence of Lucas converges - like the sequence of Fibonacci - towards the value of the golden number 1.618033 ... However, its convergence is significantly less rapid than that of the Fibonacci series. It therefore seemed useful to analyze also the impact of mutations of the human mtDNA genome on hypothetical resonances following this sequence of Lucas.

LUCAS : 2 1 3 4 7 11 18 29 47 76 123 199 322 521 843 1364 2207 3571 5778 **9349 15127 24476** 39603

We have figured in this series of Lucas the values to which we are interested, they are shown above in bold type.

We will limit this analysis to the study of the somatic mutations described in the table5.

Location mutation	Number of Resonance 9349	Number of Resonance 15127	Number of Resonance 24476
	5778 C+A 3571 T+G reference 42 resonances	9349 C+A 5778 T+G reference 26 resonances	15127 C+A 9349 T+G reference 56 resonances
1	41	24	93
32	42	15	59
45	42	15	59
46	41	24	93

52	41	24	93
55	41	24	93
59	41	24	93
60	41	24	93
62	41	24	94
64	42	26	56
64	42	15	59
66	41	24	93
67	41	24	93
72	41	24	93
73	42	15	58
74	41	24	93
74	41	24	93
74	42	26	56
80	42	26	56
84	42	15	58
91	42	15	58
92	41	24	93
94	41	24	93
97	41	24	93
100	41	24	93
16536	42	15	59
16531	42	15	59
16526	42	15	59
16518	41	24	93
16473	41	24	93
16464	42	15	59
16458	42	15	59
16437	41	24	93
16402	42	15	59
16398	42	15	59
16390	41	24	93
16389	41	24	93
16364	42	15	59
16356	41	24	93
16355	41	24	93
16354	42	15	59
16351	41	24	93
16323	41	24	93
16310	41	24	93

Table 11 : (A+C) / TCAG Lucas resonances for the 44 (19+25) mtDNA somatic mutations of Table5.

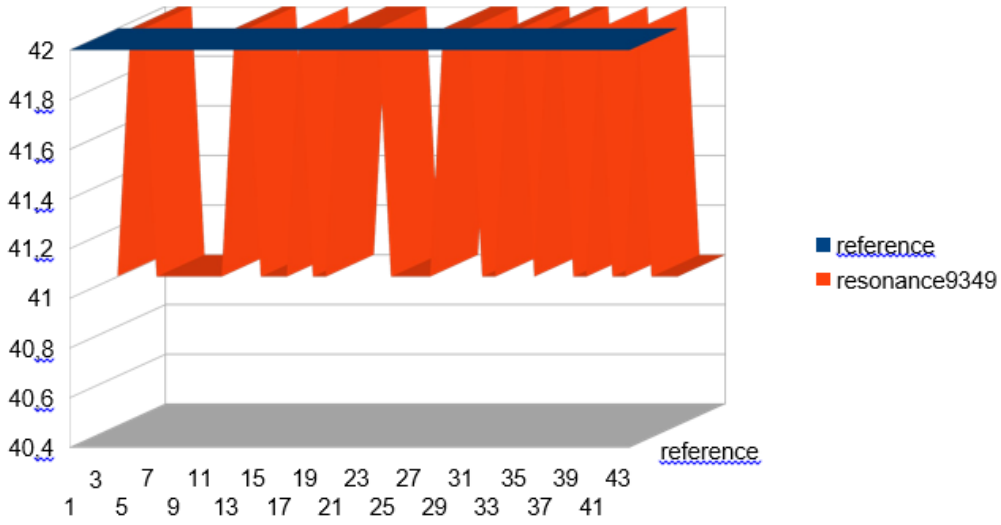

Figure 11 : : (A+C) / TCAG 9349 Lucas resonances for the 44 (19+25) mtDNA somatic mutations of Table5.

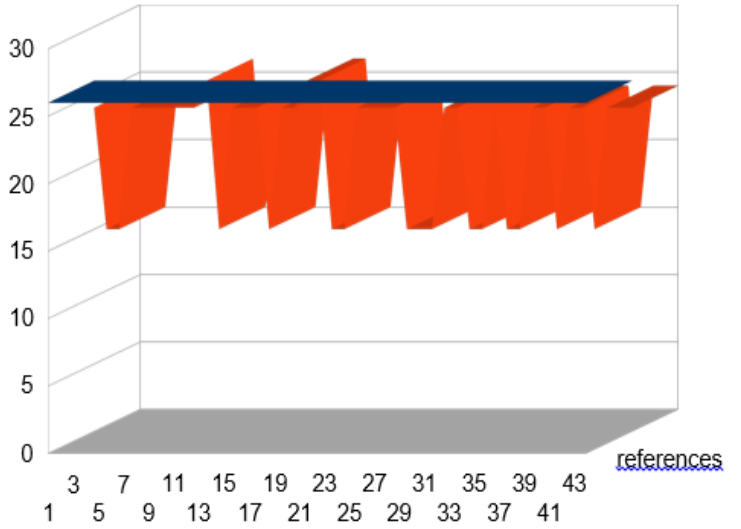

Figure 12 : : (A+C) / TCAG 15127 Lucas resonances for the 44 (19+25) mtDNA somatic mutations of Table5.

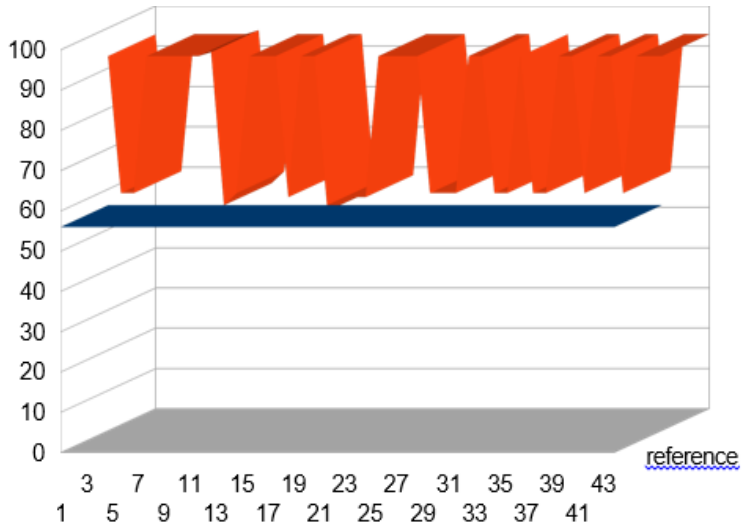

Figure 12 : : (A+C) / TCAG 24476 Lucas resonances for the 44 (19+25) mtDNA somatic mutations of Table5.

It will be noted (diametrically opposed to the study of the resonances of Fibonacci) that here resonances 9349 and 15127 DECREASE in the cases of mutations whereas the very long resonances 24476 INCREASE in the cases of mutations.

3/ Merger of 2 Fibonacci and Lucas studies :
It seemed interesting to us to merge on one and the same table both resonances of Fibonacci (Table6) and Lucas (Table11).
Recall Fibonacci and Lucas numbers :
FIBONACCI : 0 1 1 2 3 5 8 13 21 34 55 89 144 233 377 610 987 1597 2584 4181 6765 **10946 17711 28657** 46368
LUCAS :2 1 3 4 7 11 18 29 47 76 123 199 322 521 843 1364 2207 3571 5778 **9349 15127 24476** 39603
We have shown in these two sequences of Fibonacci and Lucas the values to which we are interested, they appear above in bold type.

reference		resonance934 reference		resonances10 references		resonance151 reference		resonances17 reference		resonaces244 reference		resonances 28
	42	41	10	16	26	24	8	13	56	93	152	152
	42	42	10	18	26	15	8	13	56	59	152	145
	42	42	10	18	26	15	8	13	56	59	152	145
	42	41	10	16	26	24	8	13	56	93	152	152
	42	41	10	16	26	24	8	13	56	93	152	152
	42	41	10	16	26	24	8	13	56	93	152	152
	42	41	10	16	26	24	8	13	56	93	152	152
	42	41	10	16	26	24	8	13	56	93	152	152
	42	41	10	16	26	24	8	13	56	94	152	152
	42	42	10	10	26	26	8	8	56	56	152	152
	42	42	10	18	26	15	8	13	56	59	152	145
	42	41	10	16	26	24	8	13	56	93	152	152
	42	41	10	16	26	24	8	13	56	93	152	152
	42	41	10	16	26	24	8	13	56	93	152	152
	42	42	10	18	26	15	8	13	56	58	152	145
	42	41	10	16	26	24	8	13	56	93	152	152
	42	41	10	16	26	24	8	13	56	93	152	152
	42	42	10	10	26	26	8	8	56	56	152	152
	42	42	10	10	26	26	8	8	56	56	152	152
	42	42	10	18	26	15	8	13	56	58	152	145
	42	42	10	18	26	15	8	13	56	58	152	145
	42	41	10	16	26	24	8	13	56	93	152	152
	42	41	10	16	26	24	8	13	56	93	152	152
	42	41	10	16	26	24	8	13	56	93	152	152
	42	41	10	16	26	24	8	13	56	93	152	152
	42	42	10	18	26	15	8	13	56	59	152	145
	42	42	10	18	26	15	8	13	56	59	152	145
	42	42	10	18	26	15	8	13	56	59	152	145
	42	41	10	16	26	24	8	13	56	93	152	152
	42	41	10	16	26	24	8	13	56	93	152	154
	42	42	10	18	26	15	8	13	56	59	152	147
	42	42	10	18	26	15	8	13	56	59	152	147
	42	41	10	16	26	24	8	13	56	93	152	154
	42	42	10	18	26	15	8	13	56	59	152	147
	42	42	10	18	26	15	8	13	56	59	152	147
	42	41	10	16	26	24	8	13	56	93	152	154
	42	41	10	16	26	24	8	13	56	93	152	154
	42	42	10	18	26	15	8	13	56	59	152	147
	42	41	10	16	26	24	8	13	56	93	152	154
	42	41	10	16	26	24	8	13	56	93	152	154
	42	42	10	18	26	15	8	13	56	59	152	147
	42	41	10	16	26	24	8	13	56	93	152	154
	42	41	10	16	26	24	8	13	56	93	152	154
	42	41	10	16	26	24	8	13	56	93	152	154

Table 12 : Comparative analysis of Fibonacci and Lucas resonances (A+C) / TCAG for the 44 (19+25) mtDNA somatic mutations of Table5

Now, the 3 figures below compare 2 to 2 the results for neighboring Fibonacci and Lucas numbers.

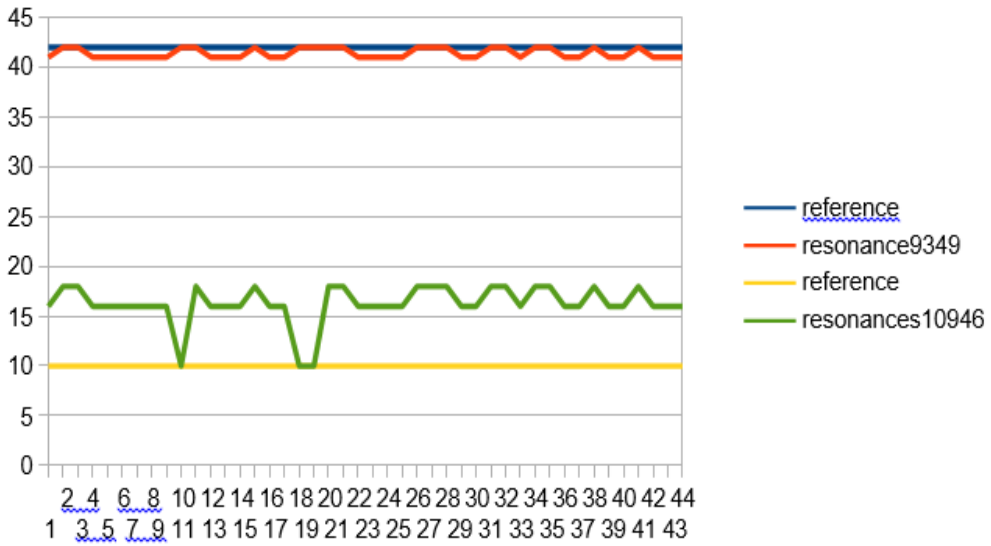

Figure 13 : Comparative analysis of Fibonacci (10946) and Lucas (9349) resonances (A+C) / TCAG for the 44 mtDNA somatic mutations of Table5.

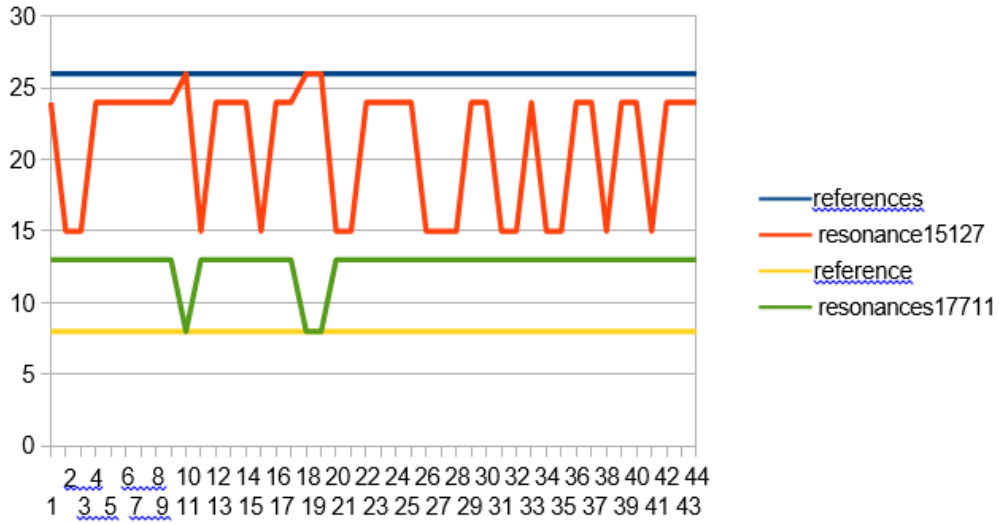

Figure 14 : Comparative analysis of Fibonacci (17711) and Lucas (15127) resonances (A+C) / TCAG for the 44 mtDNA somatic mutations of Table5.

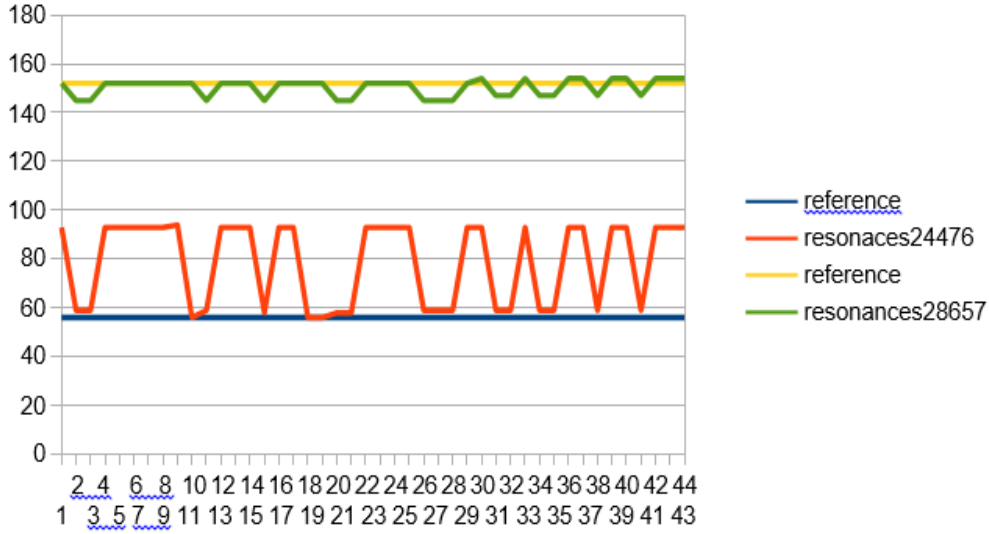

Figure 15 : Comparative analysis of Fibonacci (28657) and Lucas (24476) resonances (A+C) / TCAG for the 44 mtDNA somatic mutations of Table5.

The reader will find that these Fibonacci and Lucas couples of resonances are always always systematically opposed, some decreasing during mutations while others increase for these same mutations, and vice versa. An attempt at explanation: although the rates of convergence towards Phi = 1.618033 the golden ratio are very similar for the Lucas and Fibonacci sequences (37), these opposite effects can be explained by the kinds of "combs or

Grids "of selectivities formed by successive alternations of successive numbers of Fibonacci and Lucas, forexample:
Fibonacci : 10946 17711 28657
Lucas ; 9349 15127 24476
This suggests a certain "undulatory" nature (46) of these alternate "windows" of respective sensitivities of successively alternating numbers of Fibonacci and Lucas.

PERSPECTIVES:

One question arises: the mtDNA genome being looped back on itself, and the sequences of Fibonacci and Lucas being infinite on the other hand, it is possible (and it is even certain theoretically) that very Long circular resonances may exist. Can there be very long resonances of several million bases? We have tested this possibility by looking at the 5 reference genomes for hypothetical resonances of Fibonacci whose length could reach 15 million bases for a genome whose length is only 16000 bases. We did not find

sapiens memomt dna	10946	17711	28657	46368	75025	121393	196418	317811	514229	832040	1346269	2178309	3524578	5702887	9227465	14930352
	10	8	152	0	0	0	0	0	0	0	0	0	0	0	0	0
memone-anderthal 1																
	10946	17711	28657	46368	75025	121393	196418	317811	514229	832040	1346269	2178309	3524578	5702887	9227465	14930352
	2	16	23	92	0	0	0	0	0	0	0	0	0	0	0	0
me-modenisova1																
	10946	17711	28657	46368	75025	121393	196418	317811	514229	832040	1346269	2178309	3524578	5702887	9227465	14930352
	52	33	41	36	0	0	0	0	0	0	0	0	0	0	0	0
me-modenisova2																
	10946	17711	28657	46368	75025	121393	196418	317811	514229	832040	1346269	2178309	3524578	5702887	9227465	14930352
	10	62	10	68	0	0	0	0	0	0	0	0	0	0	0	0

Table 13 : Search for very long Fibonacci resonances for the 5 reference mtDNA genomes

Yet, over 18 years ago, in 1999 we wrote:
« Fossil NEANDERTAL's mtDNA : In 1997 then in 1999, the German researcher Svante Pääbo (13 14) analyzed two small fragments of the hyper-variable region of mtDNA taken on first Neandertalian discovered in 1856 close to Dusseldorf (and preciously preserved today). It is this specimen, old man of approximately 30000 years who was going to give birth at the end " Man of NEANDERTAL " (in memory of " Neandertal ", the area of Germany where it was discovered for the first time). While being based on the analysis of these two small DNA areas and on their level of homology to DNA from the " current Sapiens ", Dr Pääbo was going to show that NEANDERTAL and SAPIENS would be two parallel lines which would have coexisted during a few millenium. But their common stock would be much older (approximately 600000 years) and, consequently, Homo-Sapiens

would not go down from Homo-Neandertal!
The man of Neandertal would be located approximately halfway between Homo-Sapiens and our nearer close, the chimpanzee. Immense polemic in the " Evolution Scientists microcosm ", which, as each one knows, lets evolve/move its Dogmas only very slowly…Recently, in 1999, two other major publications on the subject have just established, on the one hand, than NEANDERTAL and SAPIENS had coexisted (then, probably, produced " Neandertal-Sapiens children " (15)), and, on the other hand, than NEANDERTAL was cannibal (16).

Materials and Methods : the suggested Transgene. :

Apply the following precise protocol, consider:

1.A complete genome of mtDNA from the chimpanzee " Pan Troglodyte JENNY " (GenBank X93335). This circular genome measures 16561 bases, baptize to it " CHIMP ".

2.Take the 2 fossil DNA sections of Neandertal extracted by Svante Pääbo starting from the fossil skeleton from the man from Neandertal. The co-ordinates and precise references of these 2 sequences are respectively:

i.HVR1 - 379 bases - S. Pääbo in CELL 1997 Jul 11;90(1): 19-30 (13).

ii.HVR2 - 345 bases - S. Pääbo in PNAS 1999 flight 96 pp. 5581-5585, (14).

3.Form transgene " G.M. hOmo-NEANDERTAL " by amalgamating the genome [1] of the chimpanzee and the 2 sections [2.i and 2.ii] of NEANDERTAL as follows:

i) Just after base 15447 of CHIMP, to replace the 376 following bases by 379 bases HVR1 of the NEANDERTAL.

ii) Just after base 16050 of CHIMP (original), to replace the 335 following bases by 345 bases HVR2 of the NEANDERTAL.

The new " transgenome " thus trained, " G.M. hOmo-NEANDERTAL " account now 16574 bases (instead of the 16561 initial bases).

Results :

This hybrid DNA is circular. One can seek there the "DNA Supra-Code" resonances … the thousands of " resonances " of the SUPRA-CODE of DNA structures and structures the relative arrangement of bases TCAG within DNA; we recall their computing protocol: each resonance is a remarkable arrangement of a contiguous sequence of bases TCAG following a proportion of Fibonacci's or Lucas's numbers (for example, 89 bases TCAG will be subdivided in 34 bases T and in 55 bases ACG. 34 55 and 89 are three successive numbers in the continuation of Fibonacci 1 1 2 3 5 8 13
21 34 55 89 144 233…).
There because of the circular structure, in theory, resonances INFINITE LENGTH could even emerge here.../... My recent discovered led me to interest me in particular in resonances between the bases T+G on the one hand, A+C on the other hand, and the totality of bases TCAG. For a set of native mt-genomes studied (including worm-of-ground, crocodile and monkeys or human mt-genomes), I discover indeed a great number of such resonances of which the maximum length is 28657 for the man and 75025 in the case of great apes (what is equivalent to more than one turn of genome since these genomes measure all approximately 16000 bases). All these numbers 28657, 75025 etc are whole numbers belonging to the series of Lucas (1 3 4 7 11…) or of Fibonacci (1 1 2 3 5 8 13…).
What does occur if one " dopes " these genomes by the 2 fragments of NEANDERTAL? For the few twenty species which we studied, the results are very variable then unsignificant. However, the higher primates (monkeys) and the man are those at which one observes longest resonances and the greatest influence of this " Neandertal transgene ". In certain cases, even, this ancestral transgene acts like true "a dopant"... Particularly, for the genome of the chimpanzee mentioned above, " immense resonances " then will emerge : one will count even 88 hyper-resonances which will reach the length record of 2178309 bases (TWO MILLION and 178.309 bases…!). If, now, one " dopes " this transgenic genome by changing only one A base to G on a location where this type of mutation is often observed, that will be enough then to give birth to 105 resonances from 3524578 bases and 25 other resonances of 4870847 bases… Then, there are immense resonances reaching nearly FIVE MILLION BASES… what, for a genome of 16574 bases of circumference, is equivalent to nearly 294 turns of the genome ! If we add that this phenomenon probably corresponds to properties of circulation of ELECTRONS, there gradually, between the bases…
But how thus of so gigantic resonances they could emerge?
If we have curiosity to enter the respective amounts of bases TCAG composing this genome, and, particularly, respective sums T+G on the one hand and A+C on the other hand, one will note that ratios (T+C+A+G)/(A+C) and (A+C)/(T+G) all the more approach exactly the Golden section PHI=1.618033989... which resonances become increasingly long... For example, this ratio, for the mtDNA related to the current chimpanzee and to the current human mt-DNA genomes is worth respectively 1.612 (chimpanzee) and 1.608 (man), values already very

close to Phi=1.618. Then, it appears that , in the "ideal" case of the " G.M. hOmo-NEANDERTAL " trans-genome, who counts 16574 bases, these bases are distributed in a quasi ideal way in 10244 bases AC and 6330 bases TG.
Consequently, reports/ratios:
TCAG / AC = 16574/10244 = 1.617922 and AC / TG = 10244/6330 = 1.618325
All that is quite close to the ideal ratio of the Golden section Phi=1.618033989. It does not miss, in fact, that only one base G or T more (and a base A or C in less) " to perfect " this ratio. We have find the OPTIMAL TCAG balancing point: It is, very precisely, which occurred when one reached a length close to FIVE MILLION BASES by doping transgene of only one change A to G (one reached ratio 1.618080 then).
What to think of a so beautiful Clock-like sophisticated mechanism ? »
18 years later, this catastrophe scenario became possible thanks to the CRISPR technology which could realize such manipulation worthy of the most illustrious novels of science fiction (17).
Also in 1999 we carried out another study on the mtDNA, it was never published, it consisted of looking for resonances of the Fibonacci type on the bases "G". For example, search for **987** bases "G" in a contig of length **6765** bases T C A or G. Here, **987** 1597 2584 4181 **6765** are successive numbers of the Fibonacci sequence.
We then found very large amounts of such resonances that we also correlated with the somatic mutations of mtDNA associated with various diseases.
Here is an overview, a short excerpt from this 1999 study:
*We report here a set of sixteen "cross-diseases" examples where small localized mutations in the D-loop areas (five changes and one deletion within bases 16xxx region) or various others referenced to be related to Mitochondrial Diseases, destroy partially a set of long range high level structures (lenght 6765 bases for a 16569 bases lenght genome**). These "RESONANCES" are particular proportions between the number of G bases (987) and the total bases number in the resonance (6765), where 987 and 6765 are values of the "FIBONACCI's integer numbers serie"**. The following figure summarizes this results:*

Reference Line number	Disease	Detail of Mutation	Kind of Mutation	Source/ Reference (18 19 20 21)	Number of Bases Mutations	Number of "6765 long resonances"
1/ "open" linear 16549bp mtDNA	Normal Mt-DNA	No Mutation	No Mutation	Sequence Anderson et al	0 mutation	17
2/ "closed" circular 16549bp mtDNA	**Normal Mt-DNA**	**No Mutation**	**No Mutation**	**Sequence Anderson Et al**	**0 mutation**	**184**
3/Mutations in D-loop Uncoding Area region	No disease Referended (hyper- variability)	6 Mutations: 5 changes, 1 delete	16171 → 16327 punctual mutations	Simulation	6 mutations (5 changes, 1 delete)	**103**
4/ ADPD-3196A	ADPD-Alzheimer/ Parkinson	G → A	r-RNA 16S	"Mitomap" Database	1 change	**109**
5/ LHON-15812A	LHON	G → A	Missense	"Mitomap" Database	1 change	**116**
6/ LDYS-14459A	LHON/ Dystonia	G → A	Missense	Wallace In Science	1 change	**152**
7/ ADPD-5460A	AD Alzheimer	G → A	Missense	"Mitomap" Database	1 change	194
8/ MELAS-3243G	MELAS/ Diabetes Mellitus	A → G	t-RNA Leu	Wallace In Science	1 change	**102**
9/ FICP-4269G	FICP	A → G	t-RNA Ile	"Mitomap" Database	1 change	**102**
10/ CPEO-5692G	CPEO	T → G	t-RNA Asn	" " "	1 change	**166**
11/ LHON-4136G	LHON	A → G	Missense	" " "	1 change	**102**
12/ ADPD-3397G	ADPD	A → G	Missense	" " "	1 change	**102**
13/ Caucasian people 4-mutations	LHON	4216 T→C 13708G→A 14484T→C 15257G→A	Missense	" " "	4 changes	**99**
14/ PEM-3271-del	PEM	3271 del T	t-RNA Leu	" " "	1 delete	185
15/ AMDF-7472-ins	PEM/AMDF	7472 ins C	t-RNA Ser	" " "	1 insert	185
16/ MM-15940-del	MM	15940 del T	t-RNA Thr	" " "	1 delete	185

Table 14 : G/TCAG Fibonacci resonances in 16 mtDNA human genome mutations analysed in 1999.

DISEASES ABBREVIATIONS:
LHON *(Leber Hereditary Optic Neuropathy) /* ***AD*** *(Alzheimer's disease) /* ***ADPD*** *(Alzheimer's disease and Parkinson's disease) /* ***MM*** *(Mitochondrial Myopathy) /* ***CPEO*** *(Chronic Progressive External Ophtalmoplegia) /* ***FICP*** *(Fatal Infantile Cardiomyopathy Plus a MELAS-associated cardiomyopathy) /* ***MELAS*** *(Mitochondrial Encephalomyopathy, Lactid Acidosis, add Stroke-like episodes) /* ***PEM*** *(Progressive Encephalopathy) /* ***DMDF*** *(Diabetes Mellitus + DeaFness)*
We had here a large number of G / TCAG resonances generally destroyed by different mutations cases (in bold letters). What about the resonances (A + C) / TCAG discussed earlier in this article?

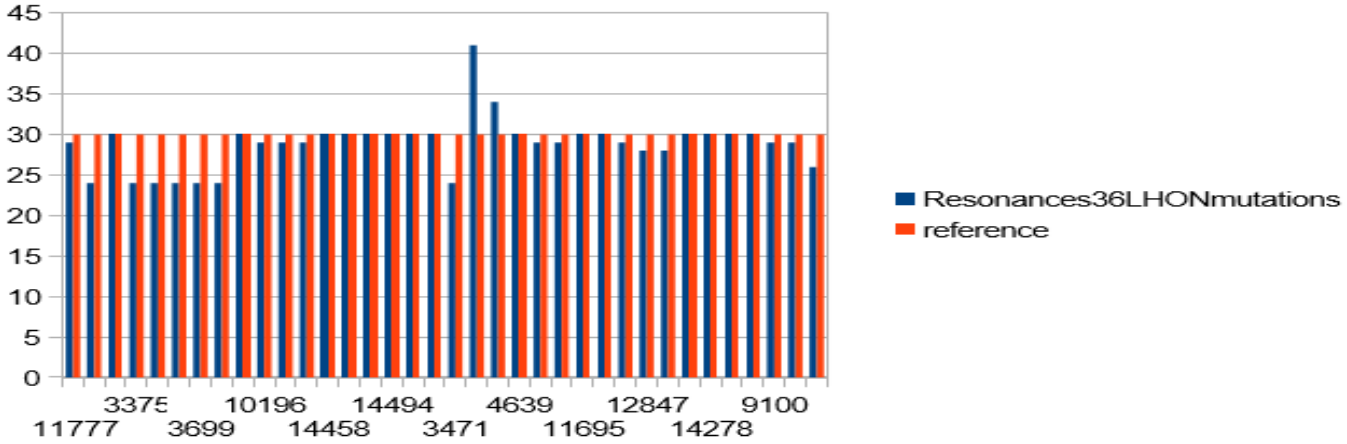

Figure 16: Example of C+A / TCAG 6765 resonances for the LHON mutations (tables 7 and 8)

It is thus observed that resonances of the mtDNA on lengths of Fibonacci of 6765 bases may be sometimes of type G / TCAG or sometimes of type (C + A) / TCAG.
The questions that we will now ask ourselves: "can there exist resonances that are simultaneously of type G / TCAG and type (C + A) / TCAG.
This would be all the more interesting since in (22) it has been demonstrated the possibility of some sort of electrical flux traveling through the bases "G" in the DNA. If this DNA is further looped back on itself, this electrical property could even give rise to "electrical oscillator" kinds!

The search for Fibonacci «Hyper Constraints Super Reonances
Let us recall the values of the Fibonacci sequence:
0 1 1 2 3 5 8 13 21 34 55 89 144 233 377 610 987 1597 2584 4181 6765 10946 17711
28657 46368 75025 121393 196418 317811
We then tried the following test:
Look for resonances that would obey simultaneously the two types of independent constraints analyzed here: 1 / (C + A) / TCAG resonances on the one hand
2 / G / TCAG resonances on the other hand Then we would have:
For populations in the following Fibonacci numbers: 987 1597 2584 4181 6765...
If the region has 6765 contiguous TCAG bases, AND
4181 (C + A) bases
THEN, it will also necessarily count 2584 bases (T + G)
AND IF
These 2584 bases (T + G) Are subdivided into
987 bases G AND
1597 bases T
THEN, we will claim to have discovered a ***"super resonance hyper constraint"*** long of 6765 bases ...
Do such resonances exist? In the case of the mtDNA genome of SAPIENS, there are 7 hyper resonances of 6765 bases ... Here is the detail and positions and TCAG distributions of these resonances:
T C A G
1597 2043 2138 **987**

1597 2043 2138 **987**
1597 2044 2137 **987**
1597 2044 2137 **987**
1597 2044 2137 **987**
1597 2045 2136 **987**
1597 2044 2137 **987**

It will be noted that in these 7 resonances, T and G are Fibonacci numbers (shown in bold) as well as the sum (A + C).
The starting addresses of these resonances are: 14753 14754 14755 14756 14757 14758 14759
It will be noticed here that these resonances can exist only thanks to the rebouche nature of the genome: in effer 14753 + 6765 > 16568 the length of the genome mtDNA.
What about the other 4 genomes of the Chimpanzee, Neanderthal and Denisova1 and Denisova2?

	Genome length (bases pairs)	Number of Hyper-resonances 6765
sapiens	16568	7
neanderthal1	16565	1
denisova1	16573	0
denisova2	16570	0
Chimp	16561	0

Table 15: Fibonacci « Hyper Constraints Super Resonances » in the cases of 5 reference mtDNA genomes.

It is found that only Neanderthal1 contains such resonance ...
Let us now analyze the 100 cases of mutations presented in the section «results»:

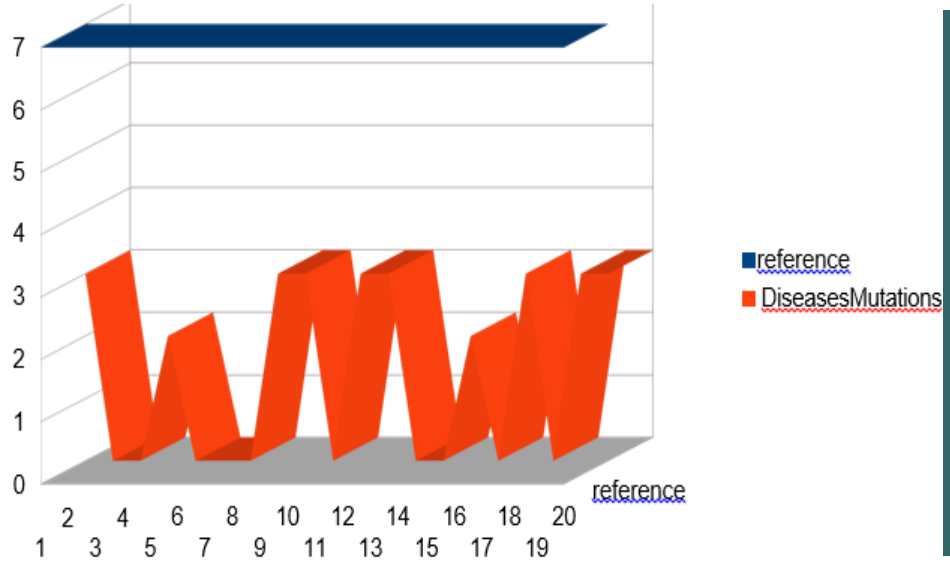

Figure 17 : Fibonacci « Hyper Constraints Super Resonances » in the case of 20 mutations of Table 2.

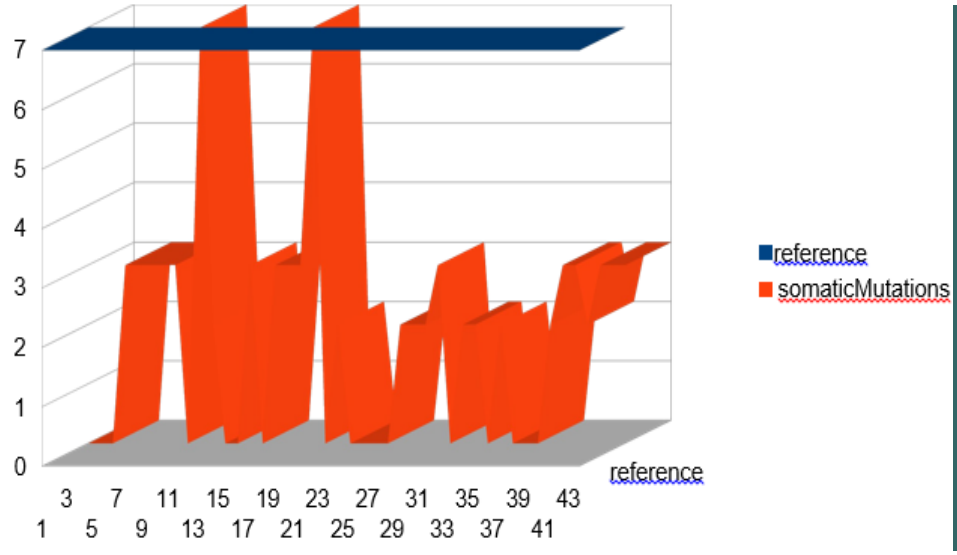

Figure 18 : Fibonacci «Hyper Constraints Super Resonances» in the case of 44 somatic mutations of Table 4

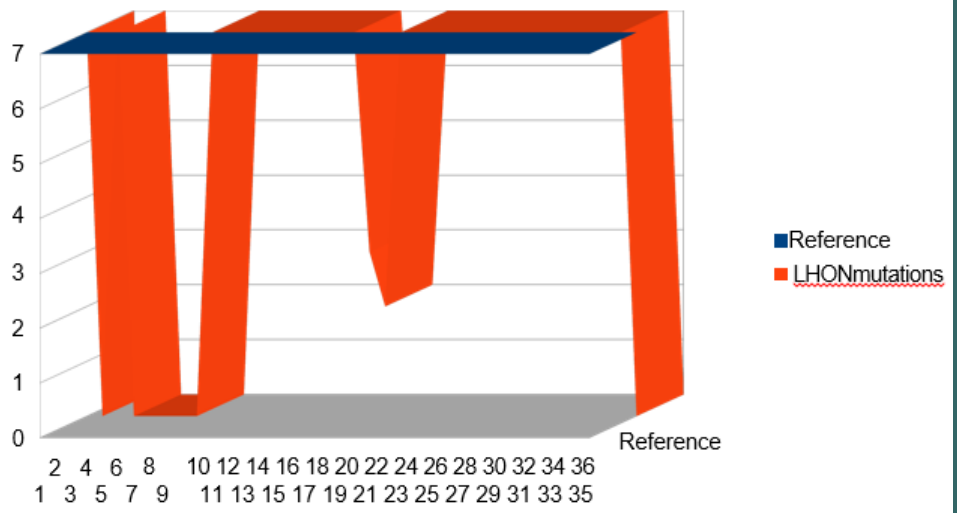

Figure 19 : Fibonacci « Hyper Constraints Super Resonances » in the case of 36 LHON mutations of Tables 7 and 8.

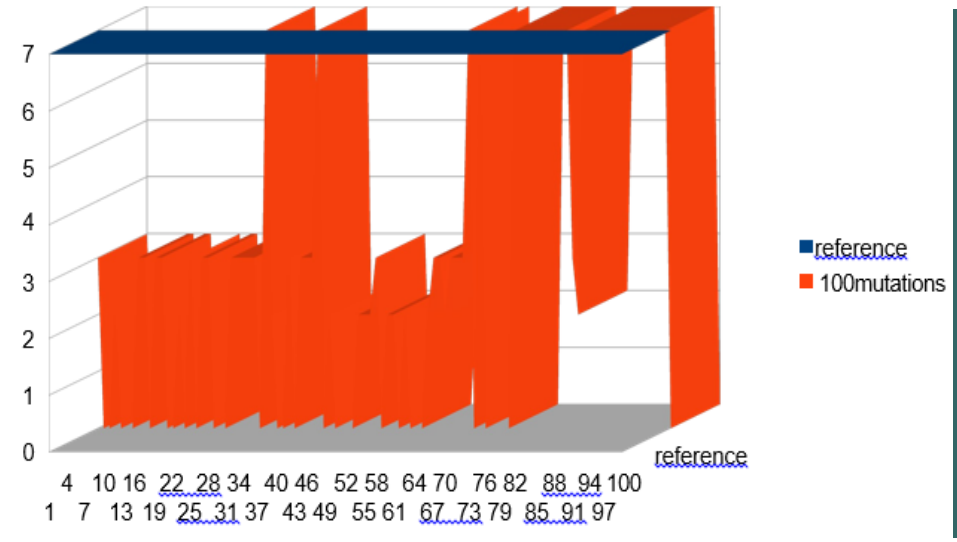

Figure 20 : Synthesis Fibonacci « Hyper Constraints Super Resonances » in the cumulated cases of 100 various mutations.

* remark :
scope of effect of these 7 resonances : 14753 + 6765 = 21518
21518 -16568 = 4950
Then these 7 resonances overlapped regions 14753 to the end of the genome (164568) and the starting region of the genoùe : 1 to 4950.

And this for 7 contiguous bases 14753 14754 14755 14756 14757 14758 14759.
We now extend this analysis to 150 cases of additional mutations, finally a total of 100 + 150 = 250 mutations cases.
Let us first study 100 new cases of somatic mutations:
Source :
http://www.mitomap.org/foswiki/bin/view/MITOMAP/MutationsSomatic

Position	Locus	Nucleotide Change	Amino Acid Change	Homoplasmy	Heteroplasmy	Cell or Tissue type	Note	References
1040	MT-RNR1	C-T	non-coding	.	.	MNGIE fibroblasts	.	1
1097	MT-RNR1	G-A	non-coding	+	-	colonic crypts	.	1
1243	MT-RNR1	T-C	non-coding	+	-	pancreatic cancer cell line	.	1
1289	MT-RNR1	G-C	non-coding	+	-	colonic crypts	.	1
1320	MT-RNR1	G-A	non-coding	-	+	normal breast	.	1
1401	MT-RNR1	G-A	non-coding	+	-	ovarian carcinoma	.	2
1406	MT-RNR1	T-C	non-coding	+	-	pancreatic cancer cell line	.	1
1474	MT-RNR1	G-A	non-coding	-	+	endometrial and ovarian tumors	.	1
1586	MT-RNR1	G-A	non-coding	-	+	colonic crypts	.	1
1676	MT-RNR2	A-G	non-coding	+	-	pancreatic cancer cell line	.	1
1721	MT-RNR2	C-T	non-coding	+	+	acute leukemia platelets, leukocytes & bone marrow	Heteroplasmic in acute leukemia, homoplasmic or absent in earlier stage.	1
1738	MT-RNR2	T-C	non-coding	+	-	colorectal tumor	.	2
1811	MT-RNR2	A-G	non-coding	+	-	head/neck tumor	.	2
1831	MT-RNR2	G-A	non-coding	-	+	colonic crypts	.	1
1952	MT-RNR2	T-C	non-coding	+	-	ovarian carcinoma	.	2
1967	MT-RNR2	T-C	non-coding	-	+	colorectal tumor	.	2
2015	MT-RNR2	G-A	non-coding	+	-	pancreatic cancer cell line	.	1
2056	MT-RNR2	G-A	non-coding	+	+	bladder tumor, acute leukemia platelets/leukocytes/bone marrow	Heteroplasmic in acute leukemia, homoplasmic or absent in earlier stage.	3
2222	MT-RNR2	T-C	non-coding	+	-	pancreatic cancer cell line	.	1
2233	MT-RNR2	T-A	non-coding	.	.	MNGIE fibroblasts	.	1
2275	MT-RNR2	T-C	non-coding	-	+	colonic crypts	.	1
2299	MT-RNR2	T-A	non-coding	-	+	colorectal tumor	.	2
2445	MT-RNR2	T-C	non-coding	+	-	bladder tumor.		2
2643	MT-RNR2	G-C	non-coding	-	+	colonic crypts	.	1
2664	MT-RNR2	T-C	non-coding	+	-	lung tumor	.	2
2680	MT-RNR2	T-C	non-coding	-	+	endometrial and ovarian tumors	.	1
2756	MT-RNR2	C-T	non-coding	.	.	Pituitary adenoma	.	1
2805	MT-RNR2	A-T	non-coding	+	-	pancreatic cancer cell line xenograf, MNGIE fibroblasts	.	2
2815	MT-RNR2	G-A	non-coding	-	+	colonic crypts	.	1
2905	MT-RNR2	A-G	non-coding	+	-	pancreatic cancer cell line	.	1
2916	MT-RNR2	G-A	non-coding	-	+	colonic crypts	.	1
2923	MT-RNR2	G-A	non-coding	+	-	prostate tumor	.	2
2998	MT-RNR2	C-CT	non-coding	+	-	lung tumor	.	1
3014	MT-RNR2	G-A	non-coding	+	-	colonic crypts	.	1
3054	MT-RNR2	G-A	non-coding	+	-	bladder tumor.		2
3094	MT-RNR2	G-A	non-coding	-	+	colonic crypts	.	1
3232:3236	MT-TL1	TAAG-T	non-coding	-	+	elderly muscle	3-bp deletion	1
3242	MT-TL1	G-A	non-coding	nr	nr	elderly brain	.	1
3243	MT-TL1	A-G	non-coding	+	+	elderly brain, elderly muscle, colon tumor, oncocytoma	.	5
3244	MT-TL1	G-A	non-coding	+	+	elderly brain,gastric carcinoma, lung tumor, thyroid oncocytoma	.	4
3308	MT-ND1	T-C	M-T	+	-	colorectal tumor	.	2
3323:3588	MT-ND1	(N)ins	multiple	-	+	renal cell carcinoma 264-bp deletion, alternate position 3326:3591		1
3357	MT-ND1	G-A	syn	+	-	prostate tumor	.	2
3386	MT-ND1	T-C	I-T	-	+	MNGIE tissues	.	1
3394	MT-ND1	T-C	Y-H	+	+	acute leukemia platelets, leukocytes & bone marrow	Heteroplasmic in acute leukemia, homoplasmic or absent in earlier stage.	1
3421	MT-ND1	G-A	V-M	+	-	pancreatic cancer cell line	.	1
3425	MT-ND1	T-C	V-A	-	+	endometrial tumor	.	1
3434	MT-ND1	A-G	Y-C	+	-	prostate tumor	.	2
3436	MT-ND1	G-A	G-Ter	-	+	head/neck tumor	.	1
3470	MT-ND1	T-C	L-P	-	+	endometrial tumor	.	1
3480	MT-ND1	A-G	syn	+	-	prostate tumor	.	2
3487	MT-ND1	C-T	syn	.	.	pituitary oncocytoma	.	1

3505	MT-ND1	A-G	T-A	+	-	pancreatic cancer cell line, prostate tumor	.	3
3526	MT-ND1	G-A	A-T	+	-	thyroid tumor	.	2
3566:3571	MT-ND1	C(6)-C(7)	frameshift	+	-	colorectal tumor, oncocytoma	.	3
3571	MT-ND1	C-del	frameshift	+	-	oncocytoma	.	1
3594	MT-ND1	C-T	syn	+	-	thyroid tumor	.	2
3653	MT-ND1	T-C	I-T	.	.	MNGIE fibroblasts	.	1
3654	MT-ND1	C-T	syn	+	-	pancreatic cancer cell line	.	1
3730	MT-ND1	T-C	Y-H	-	+	endometrial tumor	.	1
3910	MT-ND1	G-A	E-K	+	-	thyroid tumor	.	2
3918	MT-ND1	G-A	syn	.	.	breast tumor	.	2
3922	MT-ND1	G-A	E-K	+	-	head/neck tumor	.	1
3931	MT-ND1	T-C	S-P	-	+	head/neck tumor	.	1
3949	MT-ND1	T-C	Y-H	.	.	thyroid oncocytoma	.	1
3951	MT-ND1	C-T	syn	.	.	pituitary oncocytoma	.	1
3992	MT-ND1	C-T	T-M	+	-	thyroid tumor	.	2
4028	MT-ND1	T-C	I-T	.	.	MNGIE fibroblasts	.	1
4160	MT-ND1	T-A	L-H	.	.	MNGIE fibroblasts	.	1
4188	MT-ND1	A-G	syn	+	-	breast cyst.		1
4216	MT-ND1	T-C	Y-H	+	+	acute leukemia platelets, leukocytes & bone marrow	Heteroplasmic in acute leukemia, homoplasmic or absent in earlier stage.	1
4296	MT-TI	G-A	non-coding	+	-	pituitary oncocytoma	.	1
4309	MT-TI	G-A	non-coding	.	.	thyroid oncocytoma	.	1
4312	MT-TI	C-T	non-coding	+	-	thyroid tumor	.	2
4370	MT-TQ	C-T	non-coding	-	+	MNGIE fibroblasts	.	1
4398:14822	MT-TQ,MT-TM,MT-ND2,MT-TW,MT-TA,MT-TN,MT-TC,MT-TY,MT-CO1,MT-TS1,MT-TD,MT-CO2,MT-TK,MT-ATP8,MT-ATP6,MT-CO3,MT-TG,MT-ND3,MT-TR,MT-ND4L,MT-ND4,MT-TH,MT-TS2,MT-TL2,MT-ND5,MT-ND6,MT-TE,MT-CYB	(N)ins	multiple	-	+	elderly muscle	10422-bp deletion	2
4399	MT-TQ	T-C	non-coding	+	-	colonic crypts	.	1
4421	MT-TM	G-A	non-coding	-	+	elderly muscle	.	1
4446	MT-TM	G-A	non-coding	-	+	colonic crypts	.	1
4460	MT-TM	T-C	non-coding	-	+	elderly muscle	.	1
4550	MT-ND2	T-C	syn	+	-	colonic crypts	.	1
4580	MT-ND2	G-A	syn	+	-	pancreatic cancer cell line	.	1
4605	MT-ND2	A-G	K-E	.	.	head/neck tumor	.	1
4613	MT-ND2	A-G	syn	+	-	thyroid tumor	.	2
4646	MT-ND2	T-C	syn	+	-	glioblastoma	.	1
4722	MT-ND2	A-G	T-A	-	+	endometrial and ovarian tumors	.	1
4788	MT-ND2	G-A	G-Ter	-	+	colonic crypts	.	1
4811	MT-ND2	A-G	syn	+	-	pancreatic cancer cell line	.	1
4831	MT-ND2	G-A	G-D	+	+	pituitary oncocytoma	.	3
4940	MT-ND2	C-T	syn	+	-	thyroid tumor	.	2
4985	MT-ND2	A-G	syn	+	-	thyroid tumor	.	2
4986	MT-ND2	A-C	T-P	-	+	oral cancer	.	1
4986	MT-ND2	A-G	T-A	-	+	colonic crypts	.	1
5026	MT-ND2	A-G	H-R	-	+	oral cancer	.	1
5132:5134	MT-ND2	AAA-A	frameshift	+	-	skeletal muscle - myopathy	.	3
5140	MT-ND2	G-A	S-N	+	-	colonic crypts	.	1
5164	MT-ND2	G-A	R-H	-	+	colonic crypts	.	1
5198	MT-ND2	A-G	syn	+	-	glioblastoma	.	1
5212	MT-ND2	T-C	L-P	+	-	endometrial tumor	.	1
5231	MT-ND2	G-A	syn	+	-	endometrium control tissue	Normal in paired tumor tissue	1
5251	MT-ND2	T-del	frameshift	+	-	parotid oncocytoma	.	1
5260	MT-ND2	G-A	W-Ter	+	-	parotid oncocytoma	.	1
5298	MT-ND2	A-G	I-V	+	-	papillary thyroid carcinoma	.	1
5408	MT-ND2	A-del	frameshift	+	-	papillary thyroid carcinoma	.	1
5480	MT-ND2	A-C	syn	-	+	aged substantia nigra neurons	.	1
5517	MT-TW	T-C	non-coding	.	.	MNGIE fibroblasts	.	1
5521	MT-TW	G-A	non-coding	+	-	lung tumor, oncocytoma	.	3

Table 16: Analysing 100 new cases of somatic mutations by **Fibonacci « Hyper Constraints Super Resonances ».**

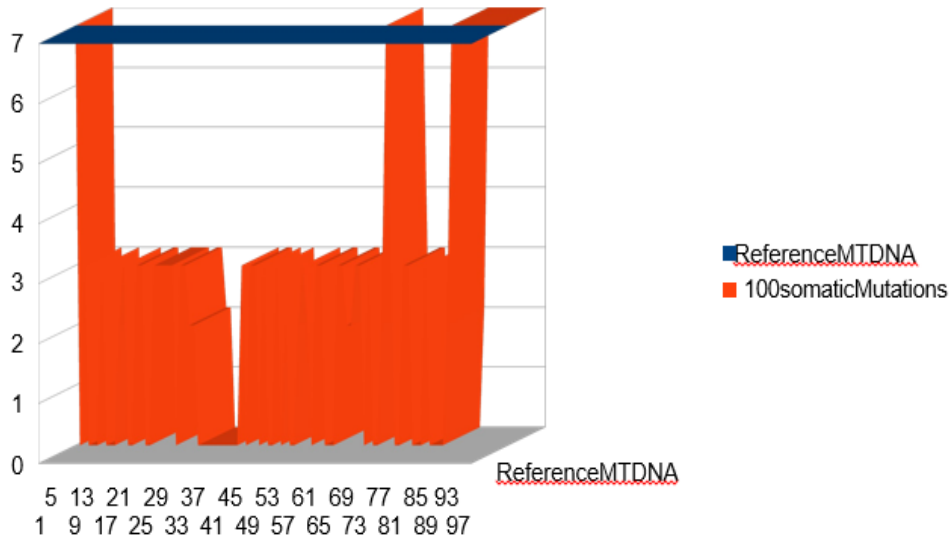

Figure 21 : Fibonacci « Hyper Constraints Super Resonances » for these 100 new cases of somatic mutations.

Then we complete by studying 50 other new cases located in the hypervariable region of mtDNA genome:

MT-CYB 15842	A-T	L-L	.	.	breast tumor	.	1
	MT-CYB	A-d	frameshift	.	.	breast tumor	. 1
15842	MT-CYB	A-T	M-L	.	.	breast tumor	. 1
15844	MT-CYB	A-C	M-I	.	.	breast tumor	. 1
15849	MT-CYB	C-A	T-N	.	.	breast tumor	. 1
15849	MT-CYB	C-T	T-I	.	.	breast tumor	. 1
15884	MT-CYB	G-C	A-P	+	-	pancreatic cancer cell line	. 1
15956	MT-TP	T-C	non-coding	-	+	MNGIE tissues	. 2
15983	MT-TP	T-C	non-coding	+	-	pancreatic cancer cell line xenograft	. 1
15995	MT-TP	G-A	non-coding	+	-	endometrial tumor	. 1
16028		T-C	non-coding	-	+	myocyte	. 1
16029		T-C	non-coding	-	+	myocyte	. 1
16033		G-A	non-coding	-	+	myocyte	. 1
16034		G-A	non-coding	-	+	ovarian tumor, myocyte, normal tissues	. 3
16035		G-A	non-coding	-	+	myocyte, normal tissues	. 2
16036		G-A	non-coding	-	+	myocyte, normal tissues	. 2
16043		A-G	non-coding	-	+	MNGIE tissues	. 1
16049		G-A	non-coding	-	+	myocyte, normal tissues	. 2
16053		Cdel	non-coding	-	+	myocyte	. 1

16054		A-G	non-coding	-	+	myocyte	. 1
16093		C-T	non-coding	+	-		
16111		C-T	non-coding	+	-		
16126		T-C	non-coding	+	-		
16134		C-T	non-coding	+	-		
				r			
16172		T-C	non-coding	-	+	MNGIE tissues, head/neck tumor back-mutation	. 3
16182		A-C	non-coding	+	+	prostate tumor	. 2
16183		A-C	non-coding	+	-	lung tumor back-mutation, prostate tumor	. 3
16183		A-del	non-coding	+	-	colonic crypts	. 1
16183		A-G	non-coding	+	-	prostate tumor	. 2
16187		C-T	non-coding	+	-	lung tumor	. 2
16188		C-CC	non-coding	+	-	hair	. 1
16189		T-C	non-coding	+	+	prostate tumor,normal buccal swab	. 5
16189		T-TT	non-coding	+	-	bladder tumor	. 1
16193		C-C(1,2,3)	non-coding	-	+	ovarian & prostate tumors, normal buccal swabs	. 4
16193		C-T	non-coding	+	-	ovarian tumor	. 1
16205		C-T	non-coding	+	+	normal buccal swab	. 2
16217		T-C	non-coding	+	-	prostate tumor	. 2
16218		C-T	non-coding	+	-	ovarian tumor	. 3
16223		C-T	non-coding	.	.	tumor	. 1
16232		C-A	non-coding	-	+	prostate tumor	. 2
16240		A-G	non-coding	-	+	endometrial tumor	. 1
16247		A-G	non-coding	.	.	MNGIE fibroblasts	. 1
16248		C-T	non-coding	+	-	ovarian tumor	. 1
16249		T-C	non-coding	-	+	prostate tumor	. 2
16260		C-T	non-coding	+	-	gastric carcinoma	. 1
16265		A-C	non-coding	+	-	bladder tumor	. 2
16274		G-A	non-coding	-	+	prostate tumor	. 2
16278		C-T	non-coding	+	-	ovarian control tissue	. 2
16290		C-T	non-coding	-	+	breast tumor	. 1
16291:19291		C-T	non-coding	+	+	normal tissues	. 1
16292		C-T	non-coding	+	-	breast, ovarian, head/neck tumor	. 4
16293		A-G	non-coding	+	-	glioblastoma	. 2
16298		T-C	non-coding	+	+	prostate tumor	. 2
16300		A-G	non-coding	+	-	head/neck tumor	. 2
16304		T-C	non-coding	+	+	esophageal, breast & prostate tumors	. 4
16309		A-G	non-coding	+	+	normal buccal swab	. 2

Table 17: Analysing Fibonacci « Hyper Constraints Super Resonances » in 50 somatics mutations from hyperloop region.

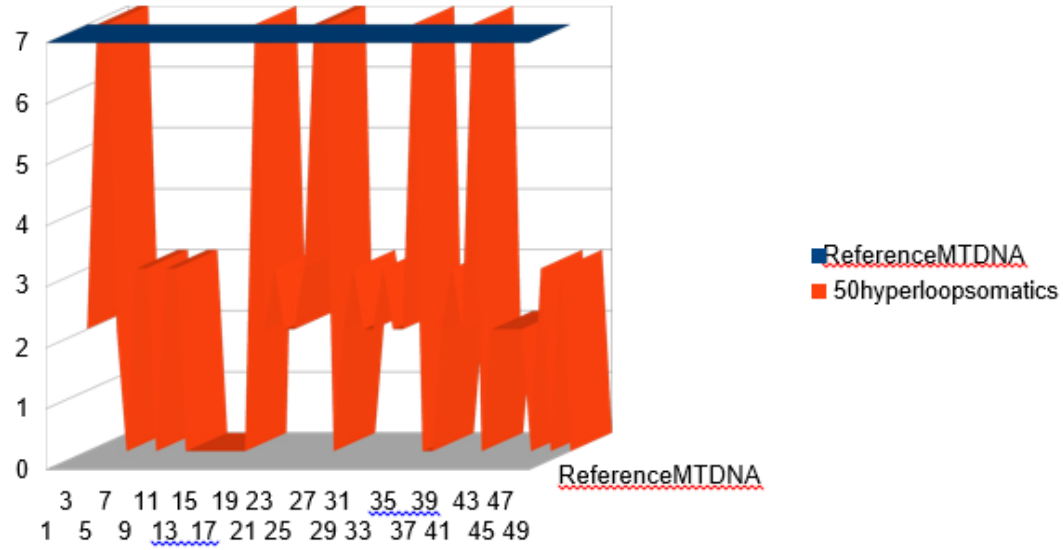

Figure 22 : Analysing Fibonacci « Hyper Constraints Super Resonances » in 50 somatics mutations from hyper-loop region.

	The 7 hyper-resonances of 6765 in the 250 analysed mutations		
	decrease	neutral	increase
1/ 20 disease mutations	20	0	0
2/ 44 somatic mutations	42	2	0
3/ all 36 LHON mutations	9	27	0
4/ 100 other somatic mutations	84	16	0
5/ 50 somatic mutations in the hyper -loop	43	7	0
total	198	52	0
Score = decrease / Total	79.2%		
Score = (decrease + neutral) / Total	100,00%		

Table 18: Final results analysing Fibonacci « Hyper Constraints Super Resonances » from 250 mutations cases.

It seems that these hyper resonances of 6765 bases are the conflicting union of the two types of concurrent and independent resonances: CA / TCAG resonances that are DECREASED by mutations on the one hand and G / TCAG resonances which are predominantly DECREASED By mutations, on the other hand. These two types of INDEPENDENT resonances thus act in the same direction under the effect of the mutations.

Final synthetic overview:
Let us therefore analyze in greater detail this mechanism of Fibonacci "Hyper Constraints Super Resonances"
It is instructive to analyze more fully the distribution and combinatorics of these "Fibonacci Hyper Constraints Super Resonances":

Fibonacci « Hyper Constraints Super Resonances »

Figure 23: Double embedded constraints of the 6765 TCAG « Fibonacci Hyper Constraints Super Resonances

Consider, for example, the first of these 7 resonances:
T C A G
1597 2043 2138 **987**
There is in fact a combinatorial of 15 possibilities of separation of the bases TCAG: All
4 TCAG bases
Combinations of bases by 3, there are 4 in number. Com-
binations of bases by 2, there are 6.
The basic combinations by 1, there are 4 of them.
How many of these combinations are Fibonacci numbers? Recall
the 2 suites of Fibonacci and Lucas:
FIBONACCI : 0 1 1 2 3 5 8 13 21 34 55 89 144 233 377 610 **987 1597 2584 4181 6765** 10946 17711
28657 46368 75025 121393 196418 317811
LUCAS : 2 1 3 4 7 11 18 29 47 76 123 199 322 521 843 1364 2207 **3571 5778** 9349 15127 24476 39603
Then :
TCAG = 6765
CAG = CA + G = 2584 + 987 = 3571 … Which is a number of Lucas
T AG = ?
TC G = ?
TCA = T + CA = 1597 + 4181 = 5778 … Which is a number of Lucas
TC = ?
TA = ?
TG = 2584
CA = 4181
CG = ?
AG = ?
T = 1597 C
= ?
A = ?
G = 987
Finally, there are 7 combinations (shown in bold in the 2 sequences of Fibonacci and Lucas above) among the possible 15 are of Fibonacci or Lucas numbers. This constitutes a very high level of constraint that applies to the relative proportions of TCAG bases involved in a "Fibonacci Hyper Constraints Super Resonances".

Another interesting remark is the following: In (38 42 43) we have demonstrated the existence of a fine- tuning on the global scale of triplet codon populations of chromosomes and even of the whole genome. Particularly, Chargaff's law (59) where (T = A) and (C = G) continues to apply to the single-stranded DNA scale. However, if we analyze the distributions T / A and C / G in a hyper resonance such as the one just described above, we observe an imbalance: indeed, C and A are very close while T / G = Phi. Hence, inside this hyper resonance, T is very different from A just as C is very different from G. The Chargaff's law is therefore not respected in the single strand of a hyper resonance. However, let us suppose that the mitochondrial DNA rewinds according to a Moebius ribbon (49), then, facing the 7 hyper resonances C = A and T / G = Phi will face 7 other hyper perfect

resonances: G = T and A / C = Phi. Then this new genome will have 7 + 7 hyper resonances perfectly respecting Chargaff's law: T = A and C = G.
Details of this Moebius strip mtDNA change :
GATCACAG .../... TCACGATG
CTAGTGTC …/... AGTGCTAC
==>
GATCACAG .../... TCACGATG linked with CTAGTGTC …/... AGTGC-TAC CTAGTGTC …/... AGTGCTAC GATCACAG .../... TCAC-GATG
Then in images :

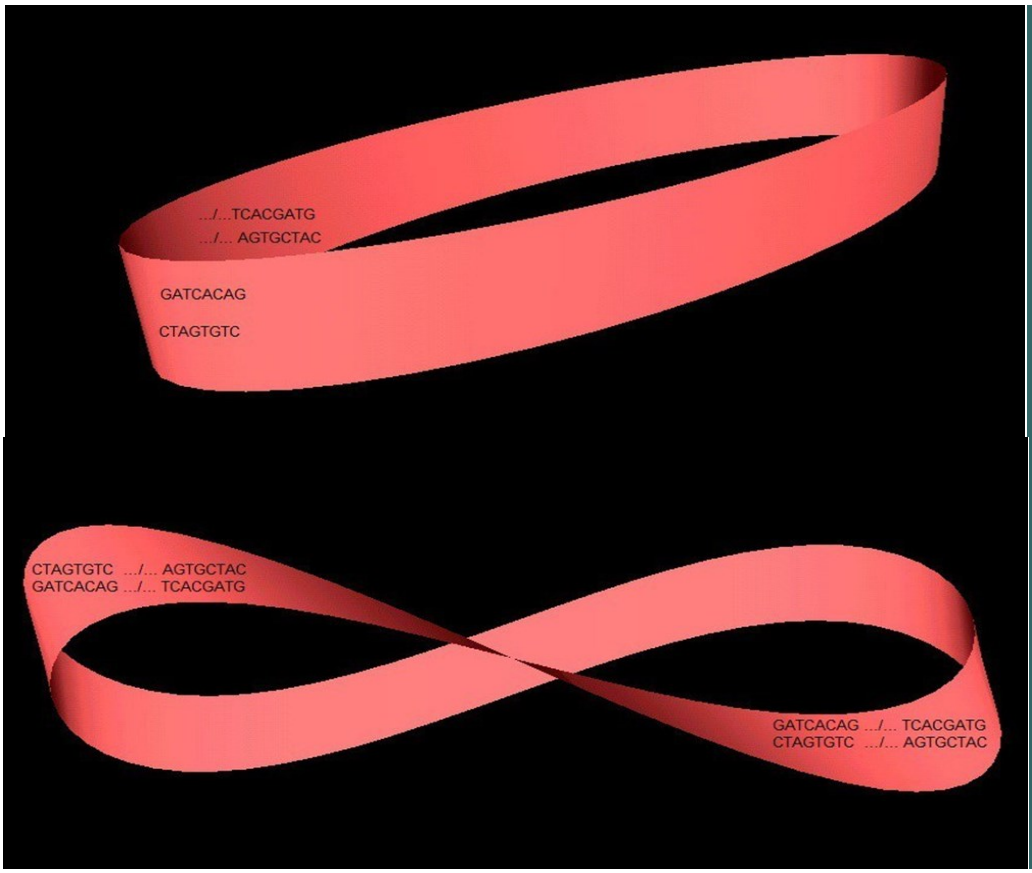

Figure 24 : Regular double stranded mtDNA genome

Figure 25 : MOEBIUS like double stranded mtDNA genome where single strand1 is linked with single strand2 and vice-versa.

Let us verify at the scale of the entire genome this same imbalance

	Dim mtDNA genome	T bases	A bases	C bases	G bases	Ratio T/A	Ratio C/G	Chargaff rule T=A and C=G on single strand DNA
Circular Regular mtDNA genome	16568	4094	5124	5181	2169	0.7989852	2.3886584	No
Moebius-like ribbon mtDNA genome [4]	33136	9218	9218	7350	7350	1	1	Yes

Table 19: Chargaff rule of single stranded mtDNA genomes in regular and Moebius strip cases.

In both cases: (T + A) / (C + G) = 1.25414966. It will be noted that this value is close to 5/4 = 1.25 with an error of 0.00414966.
This Moebius ribbon-like scenario resulting from a sort of "twist of a half turn" of the DNA molecule deserves to be explored ...

CONCLUSIONS :

In research fields, it is sometimes necessary to "leave time to time"; indeed, the methods and premises of the research that has just been presented here took root as early as the end of the 1980s, so nearly 30 years ago. ..
Infinite Diversity of digital and fractal structures of DNA and genomes:
During our Artificial Intelligence research at IBM, based on our model *"Fractal Chaos"* (23, 24, 25), we demonstrated the numerical hyper-sensitivity of an artificial neural network positioned in the vicinity of Phi and subjected to perturbations of Fibonacci number type (26, 27).
The fractal architecture (28, 29), mathematics (30) and Phi the golden number are omnipresent in Nature, in humans, in DNA, and even on the atomic scale (31) ... It is a serious mistake to fall into these simplistic thesis of an omnipresence of the golden number in the DNA as well as an omnipresence of waves in the DNA...
The reality that we have discovered for more than 25 years of biomathematic exploration of DNA is much more subtle:
Phi the golden ratio (32,33,34,35,36) and the Fibonacci numbers never appear in the same form according to the scale and level of genetic information studied:
In 1991 (37) we discovered sets of Fibonacci numbers structuring the proportions of bases TCAG within the genes sequences as well as small genomes dense in genes such as those of bacteria or, specifically, mtDNA
... but these proportions called *"resonances"* are absent in junk-DNA uncoding chromosomes regions.
In 1997 (38,39) we discovered that a numerical law of projection of the atomic masses of the nucleotides, bioatoms and amino acids, law based on Pi and Phi, unifies the 3 languages of the genetics that are DNA, RNA, and amino acids.
In 2009 (40, 41) we demonstrate that the fractal texture of the above unified genomic and proteomic images is manifested in the form of periodic discrete waves.
Finally, from 2010 (42, 43) we publish various articles demonstrating that the golden ratio controls and finely adjusts the proportions of triplets codons to the scale of the entire human genome.
This multi-level diversity of Phi is as astonishing as it is radiant ...
For example, facing the *"pentade"* formed by the five discoveries presented in this article on the one hand, in (44, 45, 46, 47) on the other hand we can only remain amazed:
-In "The Human Genome Optimum: a numerical universal law control of all chromosomal deletions involved in human cancers" (45) we show that there is a sort of HGO (human genome optimum) uniting the entire human genome. This HGO will then allow the discovery of a universal law guiding all the LOH deletions implied in the cancers.
-In "Humans and Primates Chromosomes4 Fractal CODES: periodic stationnary waveforms charaterizing and differentiating Neanderthal and Sapiens whole chromosomes DNA sequences" (46) we show a sort of hierarchy classifying the 24 human chromosomes. One of them, the chromosome4 would be a kind of leader, "lighthouse" ... and this lighthouse vibrates to the proportions of Phi, the numbers of Lucas and Fibonacci.

4 Note: this construction of a Moebius genome requires starting the genome not at the conventional address 1 but at address 14750, for example, so that hyper resonances do not overlap on either side of the boundary between Two copies of the genome, thus the only copy of the genome will contain the 7 resonances while the complementary copy extending this first copy will also contain these 7 resonances.

Finally, in (44) we discover more strange still: Phi and the numbers of Fibonacci and Lucas no longer appear explicitly. They hide behind a subtle interference, hiding behind a spectrum of numerical periods in the appearance of any numbers.
Our intuition is that there is a link, "dialogues" between these three heterogeneous but subtle disparate mechanisms that are *mathematics, fractals, and the numbers of Fibonacci, Lucas, and Golden ratio.*
Thus, in revisiting here the *"supracode of DNA"* discovered since the beginning of the 90s, as Professor Luc Montagnier baptized it (48), here we "rewind" this vast trip around digital structures of DNA and Genomes ...
Like the mtDNA genome, would the loop be "looped" ...!
However, many questions will remain to be explored as a result of this research, for example:
-What happens if the mtDNA genome accidentally loops back into Moebius ribbon (49)?
-As C. Tomasetti demonstrates in (50), "a substantial fraction of mutations in human cancer are attributable to random errors occurring during DNA replication." So - if they affect the mtDNA genome - how could these errat-

ic somatic mutations perhaps trigger the origin ofcancers?
-How did the subtle mechanisms of human evolution lead to Sapiens (44, 47, 51, 52)? What was the role of the mtDNA genome?
-However, these numerical structures that we discover here could generate phenomena of electronic (22), even oscillatory (46) and undulatory (53, 54) conductivity?
-How do these fractal structures (25, 33, 55) of DNA contribute to the dynamics of epigenetic folds?
-Finally, how this *"HomOGM" of Neanderthal* proposed as of 1999, as just presented in the Perspectives §, could today be realized thanks to the technology CRISPR (56) ... to open this era of fusion between genetic man and AI (Artificial Intelligence) so much desired by transhumanists (57, 58)?
Finally, the major fact of this research is the following: how and why - systematically - mtDNA mutations associated with pathogenic cases - NEVER lead (100% of the cases studied) to a reduction in long resonances (C + A) / (T + G) ... while « Hyper Constraints Super Resonances » decrease in 100% of the 250 cases of pathogenic mutations analyzed? What happens then in these pathogenic cells whose mitochondrial genome would seem more "optimal"? This genomic optimality leads to an energetic over-functioning of the mitochondria of this pathogenic cell (60), which could explain the extreme pathogenicity and the disturbances observed in these pathogenic cells, especially in the cases of this cancerous cells, Beyond the theoretical aspect of this article, it is indeed the field of potential applications that will have to be explored tomorrow ...
Another interesting topic that should be studied is the possible INTERACTION between the nuclear genome and the human mitochondrial genome. Indeed, it has been demonstrated (61) that in certain cancer cells, fragments of mtDNA migrate to certain chromosomes of the nuclear genome. Effectively, Mitochondrial genomes are separated from the nuclear genome for most of the cell cycle by the nuclear double membrane, intervening cytoplasm, and the mitochondrial double membrane. Despite these physical barriers, Dr Young Seok Ju et al. (61) show that somatically acquired mitochondrial-nuclear genome fusion sequences are present in cancer cells. Remarkably, mitochondrial-nuclear genome fusions occur at a similar rate per base pair of DNA as interchromosomal nuclear rearrangements, indicating the presence of a high frequency of contact between mitochondrial and nuclear DNA in some somatic cells.

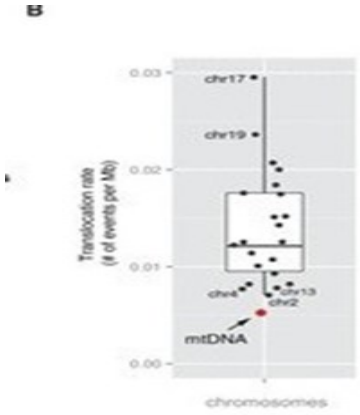

Figure 26 :
from Fig5 in ref (61) http://m.genome.cshlp.org/content/25/6/814/F5.expansion.html

Particularly, in the part B of Figure 26 from (61) are represented frequencies of somatic nuclear mtDNA integrations compared to the frequency between autosomes (chromosomal translocation). We note that Chromosomes classification (chr4, 13, 2, …/... 17 19) are in accord with the chromosomal hierarchy classification that we demonstrate in published paper (39) and in future paper (46).

It is then interesting to ask whether there is no relationship between the proportions of Fibonacci observed on the one hand, here in the mtDNA genome, and on the other hand, in certain chromosomes of the nuclear genome?
Indeed in (45), we will demonstrate that at the scale of the entire human chromosome4 and chromosome13, the ratio (C + A) / G + T) = **1 / Phi.**
On the other hand, in the 152 resonances 28651 (C + A) / (T + G) of the table1 and in the 7 "Fibonacci Hyper Constraints Super Resonances" 6765 (C + A / (T + G) = **Phi** the Golden ratio.
Now, we know that **Phi - (1 / Phi) = 1**.
Hence, there may be hypothetical "information couplings", the nature of which would be undulatory (46, 53) between, on the one hand, this famous chromosome4 and, on the other hand, these specific resonances of the mtDNA genome. And this, magicked the boundaries of membranes separating these two respective genomes in the cell.

Another track of investigations is the scenarii of « physical harmonic resonance » as sugested Dr Robert Friedman « Do you think that circular mtDNA with the right number of Fibonacci resonance points could act

Figure 27 : « physical harmonic resonance » analogy scenarii (thanks picture from Dr Robert Friedman).

epigenetics then in genes expression tuning.
To summarize, we should think then research on the following situation:
Inputs: 250 cases of mtDNA mutations associated with various human diseases.
An operator: The exhaustive search for mtDNA genome "Fibonacci resonances" associated with these mutations.
A "binary" output: a common behavior of the mtDNA genome resulting from these 250 mutations disorders.

ACKNOWLEDGEMENTS :

We especially thank *Dr. Robert Friedmann* M.D. practiced nutritional and preventive medicine in Santa Fe, New Mexico, which suggested new research interest on mtDNA genome. We also thank the mathematician Pr. *Diego Lucio Rapoport* (Buenos aires), the french biologist *Pr. François Gros* (Pasteur institute,co- discoverer of RNA messenger with *James Watson* and *Walter Gilbert*) and *Pr. Luc Montagnier*, medicine *Nobel* prizewinner for their interest in my research of biomathematical laws of genomes.

REFERENCES :

1. Perez JC (1991) Chaos DNA and neuro-computers: a golden link. Speculations in Science and Technology 14: 336-346.
2. Marcer PJ (1992) Order and chaos in DNA – the Denis Guichard Prizewinner: Jean-Claude Perez. Kybernetes 21: 60-61.
3. MITOMAP: A human mitochondrial genome database, http://www.mitomap.org/MITOMAP
4. Shoffner, John M. et al., Myoclonic epilepsy and ragged-red fiber disease (MERRF) is associated with a mitochondrial DNA
5. tRNALys mutation , Cell , Volume 61 , Issue 6 , 931 – 937
6. Wallace DC; et al. (1999). "Mitochondrial DNA variation in human evolution and disease". *Gene*. 238: 211–30. doi:10.1016/s0378- 1119(99)00295-4. PMID 10570998.
7. Wallace DC. 1987. Maternal genes: Mitochondrial diseases. In Medical and experimental mammalian genetics: A perspective (ed. McKusick VA, Roderick TH, Mori J, Paul MW), pp. 137–190. A.R. Liss, New York.
8. Wallace DC, Chalkia D. Mitochondrial DNA Genetics and the Heteroplasmy Conundrum in Evolution and Disease. *Cold Spring Harbor Perspectives in Biology*. 2013;5(11):a021220. doi:10.1101/cshperspect.a021220. ,
9. https://www.ncbi.nlm.nih.gov/pubmed/24186072
10. Irina G. Shabalina et al, Improved health-span and lifespan in mtDNA mutator mice treated with the mitochondrially targeted antioxidant SkQ1, 10.18632/aging.101174 , 2017, http://www.aging-us.com/article/101174/text
11. Larsson NG1, Somatic mitochondrial DNA mutations in mammalian aging., Annu Rev Biochem. 2010;79:683-706. doi:
12. 10.1146/annurev-biochem-060408-093701.
13. Eric A. Schon et al, Human mitochondrial DNA: roles of inherited and somatic mutations, *Nature Reviews Genetics* 13, 878-890 (December 2012) | doi:10.1038/nrg3275
14. Richard E. Green et al, A complete Neandertal mitochondrial genome sequence determined by high-throughput sequencing, Cell. Author manuscript; available in PMC 2009 Aug 8. Published in final edited form as: Cell. 2008 Aug 8; 134(3): 416–426.
15. doi: 10.1016/j.cell.2008.06.021 PMCID: PMC2602844 NIHMSID: NIHMS65170, https://www.ncbi.nlm.nih.gov/pmc/articles/PMC2602844/

16. Susanna Sawyer et al , Nuclear and mitochondrial DNA sequences from two Denisovan individuals, Proc Natl Acad Sci U S A. 2015 Dec 22; 112(51): 15696–15700., Published online 2015 Nov 16. doi: 10.1073/pnas.1519905112 ,PMCID: PMC4697428 Evolution
17. M. Krings et al (1997) in "Neandertal DNA sequences and the Origin of Modern Humans", Cell, vol 90, 1-20 (July 11, 1997).
18. M. Krings et al (1999) in "DNA sequence of the mitochondrial hypervariable region II from the Neandertal type specimen", Proc. Natl. Acad. Sci. USA, vol 96, pp. 5581-5585, (May 1999).
19. C. Duarte et al (1999) in "The early upper Paleolithic Human Skeleton from the Abrigo do Lugar Velho (Portugal) and Modern Human emergence in Iberia, Proc. Natl. Acad. Sci. USA, vol 96, pp. 7604-7609 (June 22, 1999).
20. A. Defleur et al (1999) in "Neanderthal Cannibalism at Moula-Guercy, Ardèche, France", Science, vol 286, 128 (October 10, 1999).
21. Fogleman S, Santana C, Bishop C, Miller A, Capco DG. CRISPR/Cas9 and mitochondrial gene replacement therapy: promising techniques and ethical considerations. *American Journal of Stem Cells*. 2016;5(2):39-52. https://www.ncbi.nlm.nih.gov/pmc/articles/PMC5043096/
22. D.C Wallace, "Mitochondrial Diseases in man and mouse", SCIENCE 283, 1482-1488 (1999).
23. D.C. Wallace and D.G. Murdock, "Mitochondria and Dystonia: The movement disorder connection?", PNAS vol 96 , N° 5, 1817-1819 (1999). 20
24. C.M Koehler et al, "Human deafness dystonia syndrome is a mitochondrial disease", PNAS vol 96, N° 5, 2141-2146 (1999).
25. Anderson et al, "Sequence and organization of the human mitochondrial genome", NATURE, 290, 457-465 (1981).
26. Ratner, Mark. "Photochemistry: Electronic motion in DNA." *Nature* 397.6719 (1999): 480-481.
27. J.C Perez, De nouvelles voies vers l'intelligence artificielle: pluri-disciplinarite: auto-organisation: réseaux neuronaux , Masson Paris, 1988.
28. JC Perez, La révolution des ordinateurs neuronaux
29. “FRACTAL CHAOS” a new neural network holographic model JC Perez, JM Bertille, in Neural Networks 1, 121
30. Perez JC (1990) Digital holograms computers, concepts and applications in Neural Networks / Les Reseaux de Neurones: Biological Computers or Electronic Brains / Ordinateurs Biologiques Ou Cerveaux Eletroniques. Les Entretiens de Lyon. Proceedings of the International Conference "Les Entretiens de Lyon" on Neural Networks. Ec... (Paperback), Published December 27th 1990 by Springer, Editors René Moreau and Guy Aubert, ISBN 2-287-00051-8.
31. Integers neural network systems (INNS) using resonance properties of a Fibonacci's chaoticgolden neuron'
32. JC Perez, Neural Networks, 1990., 1990 IJCNN International Joint Conference on, 859-865
33. Pellionisz AJ, Graham R, Pellionisz PA , Perez JC (2012) Recursive Genome Function of the Cerebellum: Geometric Unification of Neuroscience and Genomics. In: Manto M, DL, *et al.* (Eds) Handbook of the Cerebellum and Cerebellar Disorders. 1st (Edn), Springer, USA.
34. Dokukin ME, Guz NV, Woodworth CD, Sokolov I (2015) Emergence of fractal geometry on the surface of human cervical epithelial cells during progression towards cancer. New J Phys 17
35. Petoukhov S (2011) Mathematics of Bioinformatics: Theory, Methods and Applications. 1st (Edn), John Wiley & Sons, USA.
36. R. Coldea, D. A. Tennant, E. M. Wheeler, E. Wawrzynska, D. Prabhakaran, M. Telling, K. Habicht, P. Smeibidl, K. Kiefer. Quantum Criticality in an Ising Chain: Experimental Evidence for Emergent E8 Symmetry. Science, Jan. 8, 2010
37. Friedman R, Cross M (2013) The Golden Ratio & Fibonacci Sequence: Golden Keys to Your Genius, Health, Wealth & Excellence. 1st (Edn),
38. Hoshin Media, USA.
39. Vaezi A, Barkeshli M (2014) "Fibonacci Anyons From Abelian Bilayer Quantum Hall States." Physical Review Letters 113.
40. S.A. Olsen, Riding the Numbers: Ratios & Resonant States of Consciousness, Sociology and Anthropology 5(1): 72-75, 2017 http://www.hrpub.org DOI: 10.13189/sa.2017.050108 , http://www.hrpub.org/download/20161230/SA8-19608211.pdf
41. Perez JC (1997) L'adn Décrypté, Resurgence publisher Liege, Belgium.
42. Perez JC (2009) Codex Biogenesis. Resurgence, Liege Belgium.
43. Perez J (2015) Deciphering Hidden DNA Meta-Codes -The Great Unification & Master Code of Biology. J Glycomics Lipidomics 5:131. doi: 10.4172/2153-0637.1000131
44. Perez JC (2011) Caminos Interdisciplinaios. Seminario CLAVE_INTER, Espacio Interdisciplinario, Univer-

sidad de la Republica Montevideo, Uruguay.
45. Perez JC (2011) Decoding Non-Coding DNA Codes: Human Genome Meta-Chromosomes Architecture. BIT Life Sciences' 3rd Annual World Vaccine Congress, Beijing, China.
46. Perez JC (2010) Codon Populations in Single-Stranded Whole Human Genome DNA Are Fractal and Fine-Tuned by the Golden Ratio 1.618. Interdisciplinary Sciences: Computational Life Sciences 2: 1-13.
47. Perez JC (2013) The "3 Genomic Numbers" Discovery: How Our Genome Single-Stranded DNA Sequence Is "Self-Designed" as a Numerical Whole. Applied Mathematics 4: 37-53.
48. Perez J.C. , 41 - « DUF1220 Homo sapiens fractal periods architectures breakthrough » , to be published 2017.
49. Perez J.C. , "The Human Genome Optimum : a numerical universal law controling all LOH chromosomal deletions involved in human cancers ", to be published 2017.
50. Perez J.C., "Humans and Primates Chromosomes4 Fractal CODES: periodic stationnary waveforms charaterizing and differenciating Neanderthal and Sapiens whole chromosomes DNA sequences
51. Perez J.C., "Global and long range fractal differences between sapiens and neanderthal geomes", to be published 2017. 48 - Rachel Fleaux, "La Musique des genes", in SCIENCES § AVENIR french magazine, April 1995.
52. Diego L. Rapoport (2016) Klein Bottle Logophysics, Self Reference, Heterarchies, Genomic Topologies, Harmonicsand Evolution. Part III. The Klein Bottle Logic of Genomics and its Dynamics, Quantum Information, Complexity andPalindromic Repeats in Evolution. Quantum Biosystems. 7(1) 107-174.
53. TOMASETTI C. et al, Stem cell divisions, somatic mutations, cancer etiology, and cancer prevention
54. SCIENCE24 MAR 2017 : 1330-1334 A substantial fraction of mutations in human cancer are attributable to random errors occurring during DNA replication. http://science.sciencemag.org/content/355/6331/1330/tab-pdf
55. Weiss, Volkmar: Das IQ-Gen - verleugnet seit 2015. Eine bahnbrechende Entdeckung und ihre Feinde. Graz: Ares2017 (The IQ-Gen - Denied since 2015. A Breakthrough Discovery and its Enemies.)
56. Marshall P (2011) Evolution 2.0. Benbella Books, USA.
57. Montagnier L, Aïssa J, Ferris S, Montagnier JL, Lavallée C (2009) Electromagnetic Signals Are Produced by Aqueous Nanostructures Derived from Bacterial DNA Sequences. Interdiscip Sci Comput Life Sci 1: 81-90.
58. Boeyens_Levendis-Number_Theory_and_the_Periodicity_of_Matter(1)
59. Lieberman-Aiden et al. Comprehensive mapping of long-range interactions reveals folding principles of the human genome. Science, 2009; DOI: 10.1126/science.1181369
60. Jun Wu et al, *In vivo* genome editing via CRISPR/Cas9 mediated homology-independent targeted integration, *Nature* (16 November 2016) | doi:10.1038/nature20565
61. Roman V Yampolskiy, On the origin of synthetic life: attribution of output to a particular algorithm, The Royal Swedish Academy of Sciences , Phys. Scr. 92 (2017), DOI : 10.1088/0031-8949/92/1/013002
62. Elon Musk's New Startup Wants to Merge Human Brains With Computers, FORTUNE, Mar 27, 2017,
63. http://fortune.com/2017/03/27/elon-musk-neuralink/
64. Chargaff rules definition, http://hvc.rutgers.edu/sites/default/files/coursefiles/courses_f12/127/protected/2012-127-Ch-12-2.pdf 60 - Smith DR. The past, present and future of mitochondrial genomics: have we sequenced enough mtDNAs? *Briefings in Functional Genomics*. 2016;15(1):47-54. doi:10.1093/bfgp/elv027.https://www.ncbi.nlm.nih.gov/pmc/articles/PMC4812591/
65. Young Seok Ju et al., Frequent somatic transfer of mitochondrial DNA into the nuclear genome of human cancer cells, Genome Research, Volume 25, Issue 6, June 2015, doi: 10.1101/gr.190470.115 *Genome Res.* 2015. © 2015 Ju et al.; Published by Cold Spring Harbor Laboratory Press , http://m.genome.cshlp.org/content/25/6/814.full.pdf